THE ASTROPHYSICAL JOURNAL, 273:458–477, 1983 October 15

THE *EINSTEIN OBSERVATORY* MEDIUM SENSITIVITY SURVEY: OPTICAL IDENTIFICATIONS FOR A COMPLETE SAMPLE OF X-RAY SOURCES[1]

JOHN T. STOCKE AND J. LIEBERT
Steward Observatory, University of Arizona
I. M. GIOIA[2], R. E. GRIFFITHS, AND T. MACCACARO[2]
Harvard-Smithsonian Center for Astrophysics
AND
I. J. DANZIGER, D. KUNTH, AND J. LUB
European Southern Observatory
Received 1982 December 2; accepted 1983 March 28

ABSTRACT

Optical identifications are presented for a statistically complete sample of 63 faint, high galactic latitude, X-ray sources from the *Einstein Observatory* Medium Sensitivity Survey. Above declination $-25°$ the X-ray sources have all been identified with the following percentages: stars (25%), active galactic nuclei (AGNs, 56%), clusters of galaxies (15%). BL Lac objects and normal galaxies account for the remaining 4%. There is no evidence for a significant population of "blank field" X-ray sources. All but one of the stellar sources appear to have ratios of f_x/f_v typical of normal stars; one cataclysmic variable is found. The AGNs are almost exclusively at low redshift ($z < 1$) and are, for the most part, similar to optically selected quasars. However, ~ 20% of the AGNs have reddish colors ($B - V \gtrsim 0.7$) and spectra whose permitted lines have prominent narrow-line components (FWHM $\lesssim 1000$ km s^{-1}). Due to their red colors and weak lines, these objects, several of which appear stellar on the POSS, would not have been easily discovered optically and may represent a new class of quasar. Also present in the sample is a pair of high redshift quasars with identical redshifts and 8 Mpc physical separation. These quasars are physically distinct (only one is a strong radio source) and are probably members of the same supercluster. The number of detected clusters of galaxies in this survey is small, but as yet there is no evidence for a deficiency of high redshift clusters as is expected if dynamical evolution of their gravitational potentials is strong. Optically they are characterized as poor clusters or compact groups of galaxies but their X-ray luminosity distribution largely overlaps with the luminosity distribution of richer clusters.

Subject headings: galaxies: clusters of — galaxies: nuclei — X-rays: sources

I. INTRODUCTION

The *Einstein Observatory* Medium Sensitivity Survey (Maccacaro *et al.* 1982, hereafter, Paper I) is an X-ray survey covering ~ 50 square degrees of the high galactic latitude sky ($|b^{II}| \geq 20°$). The sensitivity of this survey (7×10^{-14} to 5×10^{-12} ergs cm^{-2} s^{-1} in the soft X-ray band; 0.3–3.5 keV) is intermediate between the bright, all-sky surveys of *Uhuru*, *Ariel V*, and *HEAO 1* and the *Einstein* Deep Surveys (Giacconi *et al.* 1979; Griffiths *et al.* 1983). The sources detected in the Medium Survey were found "serendipitously" in the inner part ($32' \times 32'$) of the Imaging Proportional Counter (IPC) field of view. The targets of the IPC observations ranged from galactic stars to known clusters of galaxies and quasars. Approximately one-third of the serendipitous sources have been reobserved and detected with the High Resolution Imager (HRI). Particulars of the source selection process, which were necessary to avoid bias due to the targeted objects themselves, are discussed in Paper I along with a detailed discussion of the extragalactic source counts.

In this paper we present the optical identifications for this sample of sources. We undertook to identify all sources without regard to an optical limiting magnitude or to any type of prior evaluation of the optical field within the X-ray error circle. At this writing, the survey identifications are complete above declination $-25°$. Identifying a complete sample of sources is important for:

1. Determining true surface densities for the various classes of X-ray emitters (e.g., QSOs, clusters of galaxies) in the flux range surveyed,

[1]Research reported here used the Multiple Mirror Telescope Observatory, a joint facility of the Smithsonian Institute and the University of Arizona.
[2]Also from Istitutó di Radioastronomia del CNR, 40126 Bologna, Italy.

2. Evaluating the extragalactic source counts in the $\log N - \log S$ diagram and the discrete source contribution to the X-ray background,

3. Determining whether a new class of X-ray emitter with a large value of f_x/f_v exists. Such objects would remain unidentified optically due to their faint optical magnitudes (i.e., "blank fields").

In this paper, we will use the $\delta \geq -25°$ sample to draw conclusions concerning the classes of sources discovered and their basic properties. Other papers in this series specifically analyze the change in source counts as a function of X-ray flux in order to delineate the evolutionary trends for the AGNs and clusters of galaxies as X-ray emitters (Maccacaro *et al.* 1982, 1983; Stocke *et al.* 1982*a*). Herein, we present the optical counterparts of the X-ray sources (§ II), describe the identification process and its reliability (§ III), and discuss the optical properties for the various classes of identifications (§ IV). A summary of the results is given in § V.

A Hubble constant $H_0 = 50$ km s^{-1} Mpc^{-1} and a Friedmann universe with $q_0 = 0$ are assumed throughout the paper.

II. THE SAMPLE

The 63 sources detected in the *Einstein* Medium Survey and presented in Paper I are listed in Table 1 along with the optical properties for all objects inside the 90% confidence X-ray error circle.

Table 1 contains the following information:

Col. (i): The position of the X-ray centroid for each source in 1950.0 coordinates. These positions supercede those of Paper I.

Col. (ii): The 90% confidence error circle (radius) of the X-ray position. All sources were initially detected with the IPC (60″ positional accuracy or 30″ if new "reprocessing" of data is available). Subsequent HRI observations of some of the IPC fields redetected ~ one-third of the sources (10″ positional accuracy or 4″ if new "reprocessing" of data is available).

Col. (iii): The X-ray flux in ergs cm^{-2} s^{-1} in the 0.3–3.5 keV energy band. All fluxes quoted are from the IPC and are taken from Paper I.

Col. (iv): Letter designations for each optical object as they appear in the finding charts in Figure 1 (Plates 22–25). An asterisk indicates the proposed identifications for each source. Where the source identification is a cluster of galaxies, the asterisk is next to the galaxies in the cluster which were actually observed and for which redshifts were obtained. Daggers indicate sources for which notes appear at the end of Table 1.

Col. (v): Spectral classification for each object observed.

Col. (vi): Redshifts uncorrected for galactic or terrestrial motion.

Col. (vii): Visual magnitudes estimated from the Palomar Sky Survey E plates using the system of King and Raff (1977) and crudely verified by the spectrophotometry obtained in the identification process. We estimate that these magnitudes are accurate only to ± 0.5 mag and that there may be a systematic underestimate of a few tenth of a magnitude particularly for objects with $m_v \geq 19$ since the POSS E plate limit by the King and Raff (1977) procedure is $m = 20.5$, while that limit has been traditionally set ~ 0.5 mag brighter (Abell 1957). In the south, the ESO "quick blue" survey was employed for the finding charts and magnitudes.

Col. (viii): The limiting POSS E magnitudes for each field (either the magnitude of the brightest object which was not observed inside the error circle or the limit of the Palomar Observatory Sky Survey E plate ($m_v \approx 20.5$) if all objects visible on the POSS were observed).

Col. (ix): General comments, including specifically radio data taken, unless otherwise noted, from the VLA survey of this sample by Feigelson, Maccacaro, and Zamorani (1982). References to previous optical work on the proposed identifications are also given.

The finding charts for each field are shown in Figure 1. The center of each chart marks the centroid of the X-ray source. The scale is shown in the first chart. The letters on the finding charts correspond to the optical designations in column (iv) of Table 1.

As can be seen from Table 1, all sources north of $-25°$ declination have been identified. South of $\delta = -25°$ the lack of Palomar Observatory Sky Survey plates and VLA radio data conspire to make the identification process more difficult.

Hence the sources with $\delta \geq -25°$ form a complete sample of fully identified X-ray sources which can be used for statistical purposes (cf. Stocke *et al.* 1982*b*; Maccacaro *et al.* 1983).

III. THE IDENTIFICATION PROCESS AND ITS RELIABILITY

In identifying this sample of X-ray sources we used the extremely naive but safe procedure of observing all the optical objects inside, or immediately outside, the 90% confidence error circle in order of increasing magnitude until we located a plausible candidate for the identification of the X-ray source. We then continued to observe optical objects until we reached a limit at least 4 times fainter than the proposed counterpart or the limit of the POSS, whichever came first. These limiting magnitudes are listed for each field in Table 1. The "typical" values of f_x/f_v for each class of object were obtained from pointed *Einstein* detections (Vaiana *et al.* 1981 for stars; Zamorani *et al.* 1981 for quasars; Schwartz, Madejski, and Ku 1982 for BL Lacs; Henry *et al.* 1979 for the brightest galaxy in clusters of galaxies).

The spectra for the objects listed in Table 1 were obtained primarily with the Steward 2.3 m telescope plus Reticon spectrograph, MMT spectrograph, and ESO

1983ApJ...273..458S

TABLE 1

OPTICAL IDENTIFICATIONS FOR *EINSTEIN* MEDIUM SURVEY SOURCES

(i) Position	(ii) Accuracy arcsec	(iii) X-ray erg/cm/s (x10^{-13})	(iv) Object	(v) Spectral Classif.	(vi) z	(vii) m v	(viii) Limiting m	(ix) Comments
1 11 54.9 -1 32 25.8	60"	3.91	*A	AGN	.120 ±.003	19.2	20.0	
1 12 59.7 -1 47 43.7	60"	1.40	+ *A	AGN	.284 ±.001	19.8	20.5	
1 26 24.4 7 25 41.5	60"	4.82	+ *A	galaxy in cluster?	.087 ±.001	17.0	19.0	no emission lines S(6cm)= 14.7 mJy
			+ *B	galaxy in cluster?	.082 ±.001	17.5		no emission lines
			C	early M star		18.2		if id.,log(fx/fv)=2
1 35 .3 3 39 29.9	60"	2.44	*A	AGN	.637 ±.003	18.7	20.5	
1 36 20.2 6 5 50.1	60"	2.10	*A	AGN	.450 ±.001	18.6	20.5	S(6cm)= 16.3 mJy
1 44 11.8 -0 55 39.4	4"	8.09	*A	AGN	.080 ±.001	15.6	20.5	
			B	galaxy	.078 ±.001	17.5		no emission lines
4 12 27.3 -8 3 8.1	4"	22.5	*A	AGN	.037 ±.001	15.4	20.5	S(6cm)= 1.9 mJy (Steiner,Grindaly and Maccacaro,1982)
			B	late type star		18.5		
			C	galaxy	.038	18.5		no emission lines
			D	galaxy	.038	17.0		no emission lines
4 20 6.1 -38 38 52.4	60"	1.23	A	mid K		16.0	18.5	possible distant cluster of galaxies in error circle
			B	probable galaxy		18.5		
4 20 23.7 -38 59 51.9	60"	1.51	*A	K5 star		12.5	17.8	
			B	late type star		15.3		
4 20 55.1 -39 3 25.3	60"	2.01	A	late G/ early K star		18.4	20.5	
			B	late G star		18.2		
			*C	AGN	.271 ±.001	19.1		
4 38 39.1 -10 49 48.2	60"	4.51	A	late F/ early G star		14.4	20.5	
			B	late A/ early F star		14.6		
			C	G star		16.9		
			D	early/mid K star		18.1		
			E	early M star		19.0		
			+ *F	AGN	.868 ±.003	20.2		S(6cm)= 26.8 mJy
			+ *G	dMe star		16.8		
			H	early/mid K star		18.9		
4 39 18.2 -11 2 11.6	60"	2.32	A	late F/ early G star		14.4	19.0	outside error circle
			B	galaxy in cluster	.152 ±.002	17.8		no emission lines S(6cm)= 16.5 mJy
			+ *C	galaxy in cluster	~.16	18.5		no emission lines
			D	galaxy in cluster	~.16	18.8		no emission lines
4 40 1.1 -10 57 30.6	60"	2.60	*A	AGN	.279 ±.003	18.8	20.5	
			B	late G star		16.4		
			C	early K star		16.9		
			D	early K star		15.9		
4 47 9.5 -9 17 17.9	4"	2.21	A	late K star		17.5	20.5	
			B	late type star		19.1		
			*C	AGN	.946 ±.003	18.5		
4 49 24.7 18 23 44.7	4"	7.81	*A	AGN	.338 ±.003	18.5	20.5	(Stocke et al.,1982a) S(6cm)= 1.1 mJy
			B	early type star		18.0		
4 50 23.2 -18 17 00.7	4"	5.37	*A	AGN	.059 ±.001	17.8	20.5	S(6cm)= 2.6 mJy

1983ApJ...273..458S

TABLE 1—*Continued*

(i) Position	(ii) Accuracy arcsec	(iii) X-ray erg/cm/s -13 (x10)	(iv) Object	(v) Spectral Classif.	(vi) z	(vii) m v	(viii) Limiting m	(ix) Comments
5 36 23.5 -28 48 54.5	60"	1.74	A	F star		16.9	20.0	
			B	late type star		19.1		
			+ *C	galaxy	.45 ±.01	20.6		no emission lines tentative id.; distant cluster
			D	G star		16.9		
5 37 11.3 -28 34 19.4	60"	1.67	A	G star		15.1	19.5	
			B	late F star		14.2		
			C	early M star		18.7		no emission lines
			D	early M star		17.2		no emission lines
			+ *E	dMe star		18.0		H alfa in emission tentative id only
			F	Star		19.2		
			G	probable galaxy		19.5		
6 22 34.4 -52 55 14.0	60"	6.78	A	G star		17.0	19.0	field obscured by Canopus;x-ray variable (Gioia et al. 1983)
			B	late F/ early G star		18.2		
6 48 10.1 -50 42 30.0	60"	4.55	*A	K5 star		12.5	19.8	
			B	late F star		16.4		
			C	early G star		16.2		
8 9 52.7 48 9 32.7	60"	2.37	+ *A	G8-K0 star		11.6	20.5	
			+ *B	AGN	.459 ±.003	19.1		
8 34 47.3 65 12 29.3	60"	50.1	*A	G0 star		5.7	obscured	SAO 146009
8 38 38.3 13 24 38.2	60"	1.80	A	G0 Star		15.8	20.5	
			*B	AGN	.723 ±.001	19.6		
8 49 5.8 28 45 15.9	30"	1.56	A	early K Star		11.2	20.5	
			B	G star		15.4		
			C	early G star		15.4		
			+ *D	AGN	1.273 ±.003	20.2		S(6cm)= 336 mJy B2 0849+28 (Colla et al.1972)
8 49 15.6 28 29 01.9	4"	1.95	*A	AGN	.209 ±.002	20.5	20.5	
8 49 48.7 28 20 01.4	30"	2.13	*A	AGN	.197 ±.003	18.5	20.5	
			B	early M star		16.2		no emission lines
			C	late G star		16.2		
8 50 02.9 28 28 06.7	30"	1.40	A	K star		16.2	20.5	
			B	late G star		16.5		
			C	not observed		17.2		slightly outside error circle
			*D	AGN	1.273 ±.004	20.0		
			E	early K star		18.1		
			F	G star		17.1		
8 50 17.9 28 25 17.2	10"	1.30	*A	AGN	.922 ±.002	17.7	20.5	S(6cm)= 37 mJy
8 50 54.8 14 1 26.6	60"	7.74	*A	A 3 star		7.0	18.5	SAO 098202
			B	late F star		17.0		
9 3 32.8 17 11 28.2	4"	3.32	*A	M1.5(e) star		13.0	20.5	Halfa in emission only
9 4 30.6 16 50 56.5	60"	8.70 (extended)	+ *A	galaxy in cluster	.074 ±.002	16.5	17.0	no emission lines Abell 744
9 37 49.4 11 53 17.9	60"	2.52	*A	AGN	.783 ±.003	18.6	20.5	
			B	early K star		16.0		
9 38 22.7 11 51 3.6	60"	1.23	*A	G2 star		12.5	20.0	
			B	K star		16.5		
			+ C	galaxy	.128 ±.001	18.0		no emission lines
9 39 49.9 -23 29 30.3	60"	1.39	*A	F0 star		8.2	20.0	SAO 177863
			B	B star		17.8		

1983ApJ...273..458S

TABLE 1—*Continued*

(i) Position	(ii) Accuracy arcsec	(iii) X-ray erg/cm/s -13 (x10)	(iv) Object	(v) Spectral Classif.	(vi) z	(vii) m v	(viii) Limiting m	(ix) Comments
12 1 32.8 28 23 50.5	60"	7.98 (extended)	*A	galaxy in cluster	.167 ±.001	16.9	17.5	no emission lines
12 7 55.1 39 45 48.5	4"	14.9	+ *A	AGN	~1.84	20.3	20.5	spectrum from H.Arp (De Ruiter,Willis and Arp,1977) S(6cm)= 5.8 mJy
12 8 18.1 39 45 03.6	4"	3.16	*A	galaxy	.0224 ±.0002	13.0	20.5	NGC4156(Elvis et al. 1981)
12 8 42.5 39 28 20.1	60" (extended)	2.59	A	F star		10.7	20.5	outside x-ray error circle
			+ *B	galaxy in cluster	.34 ±.02	19.8		no emission lines S(6cm)= 1.4 mJy
			C	late F/ early G star		18.8		
12 23 33.2 25 22 48.8	60"	7.48	*A	AGN	.067 ±.001	16.3	20.5	
12 40 52.9 3 12 15.1	4"	17.1	*A	cataclysmic variable		16.5	20.5	
12 47 3.5 -5 48 24.5	4"	16.8	*A	G 5 star		9.0	20.5	SAO 138983
13 27 26.4 32 8 9.4	60"	9.83	*A	AGN	.090 ±.001	17.3	19.0	
			B	early K star		17.3		
13 39 54.2 60 30 24.0	4"	5.10	*A	K2 star		14.8	20.5	
14 2 19.6 4 16 22.3	4"	11.5	*A	BI Lac		17.5	20.5	S(6cm)= 17.7 mJy (Stocke et al.1982b)
14 15 2.3 25 13 22.8	60"	1.96	A	early type star		19.5	20.5	
			*B	AGN	1.057 ±.005	20.5		
14 15 6.6 25 27 26.3	10"	1.80	*A	AGN	.560 ±.003	20.0	20.5	
14 16 14.8 25 25 4.5	60"	6.91 (extended)	*A	galaxy in cluster	.290 ±.003	18.9	20.0	no emission lines S(6cm)= 9.2 mJy
14 16 42.2 25 24 11.3	60"	1.67	A	K star		15.0	20.5	
			*B	AGN	.674 ±.003	18.7		
			C	K star		18.9		
14 54 3.0 22 32 23.4	60"	2.33	A	galaxy in cluster	.108 ±.002	17.5	19.0	no emission lines S(6cm)= 2.8 mJy
			* B	galaxy in cluster	~.11	17.8		
14 57 2.6 22 26 03.0	4"	6.69	*A	M2(e) star		13.3	20.5	hyd. lines in emis.
15 25 6.5 15 50 31.1	60"	11.3	*A	AGN	.230 ±.001	17.4	20.0	(Grindlay et al.1980)
15 28 30.7 8 45 10.0	60"	8.86	*A	F 2 star		6.5	17.0	SAO 121038
15 32 56.7 9 18 31.7	60"	9.38	*A	G 5 star		8.6	14.5	SAO 121078
			B	early K star		11.3		
15 33 32.8 14 40 59.1	4"	6.43	*A	AGN	.021 ±.002	15.9	20.5	
15 48 45.2 11 25 19.5	10"	9.04	*A	K5 star		13.5	20.5	
15 49 49.4 20 22 56.5	4"	16.5	+ *A	AGN	.250 ±.003	17.4	20.5	LB 0906 (Luyten and Miller,1956)
			B	galaxy	.135 ±.003	18.0		
16 17 56.5 17 31 33.7	4"	20.7	*A	AGN	.116 ±.001	15.4	20.5	PG Qso (Schmidt and Green,1983) Markarian 877
			B	galaxy	.10 ±.01	18.2		
			C	galaxy	.097 ±.005	16.5		

1983ApJ...273..458S

TABLE 1—*Continued*

(i) Position	(ii) Accuracy arcsec	(iii) X-ray erg/cm/s -13 (x10)	(iv) Object	(v) Spectral Classif.	(vi) z	(vii) m v	(viii) Limiting m	(ix) Comments
17 45 17.1 27 47 38.2	60"	3.12	A	A star		15.5	20.5	
			*B	AGN	.156 ±.001	18.6		
			C	G star		15.8		
17 51 2.8 70 46 16.5	10"	36.9	*A	K2-3 star		13.1	20.5	possible weak Halfa emission
19 10 32.1 67 36 38.0	60"	8.75	A	A star		14.7	20.0	
			B1	G star		15.7		unresolved on POSS
			B2	late F star		15.8		1=North, 2=South
			C	G star		14.5		
			D	early G star		16.8		
			*E	galaxy in cluster	.246 ±.005	19.0		no emission lines
			F	K star		19.1		
			G	K star		18.8		
			H	mid G star		13.9		
			I	late G star		15.1		
21 41 36.8 4 38.6	4"	3.01	*A	AGN	.410 ±.003	19.2	20.5	
22 4 3.1 -40 59 16.9	4"	12.4	*A	AGN	.231 ±.001	19.8	20.0	
22 23 39.6 -5 17 22.9	60"	2.03	A	early G star		15.0	20.5	
			*B	AGN	1.866 ±.003	18.6		
			C	K star		18.0		

Notes to Table 1

1E 0112.9−0147: The only object visible in the error circle on the POSS is a 19th mag object with narrow Hβ + [O III] in emission and H and K, G band, and Mg *b* absorption lines with $z = 0.284$. No cluster is visible on the POSS or on a deeper CCD frame (R. Schild 1982, private communication). This object is possibly an extreme example of a narrow emission line (Seyfert 2) galaxy.

1E 0126.4+0725: Shakbazian 41 is a compact group of two $M_v = -19$ galaxies plus several dwarf companions and is quite similar to the Local Group. The X-ray source could still be either a gaseous halo source or a source in the nucleus of one of these galaxies. The fainter unobserved objects are all probable group members (see also § III).

1E 0438.6−1049: This source is identified with the AGN. The X-ray contours show a slight extension toward the nearby dwarf M emission star, which is possibly a weak X-ray emitter.

1E 0439.3−1102: A cluster source; unobserved objects are probable cluster members.

1E 0536.3−2848: A possible distant cluster. The redshift is tentative.

1E 0537.1−2834: The dMe star is a tentative identification both because there are fainter candidates which have not yet been observed but which are closer to the X-ray centroid and because its f_x/f_v ratio is an order of magnitude larger than other M1.5(e) stars in Váiana *et al.* (1981).

1E 0809.8+4809: Both the star and the quasar are consistent with being the X-ray emitter.

1E 0849.0+2845: Prior to a recent reprocessing of this IPC image, both the star and the quasar were consistent with being the X-ray emitter. The new reprocessed position listed in Table 1 is ~15″ west of the quasar and excludes all objects except the quasar from the error circle. The finding chart in Fig. 1 for this field is centered at the old IPC position.

1E 0904.5+1650: A cluster source. Abell 744 richness = 0; fainter objects as yet unobserved by us are probable cluster members. A detailed analysis of this source will be published elsewhere (Huchra *et al.* 1983).

1E 0938.3+1151: Galaxy labeled C in Fig. 1 is too far from the X-ray centroid to be the X-ray source.

1E 1207.9+3945: The redshift for this AGN comes from a multichannel scanner observation by H. Arp. However, we have yet to confirm this redshift. See § IV*c* for discussion of this source.

1E 1208.7+3928: A cluster source: numerous galaxies too faint to be visible on the POSS were visible on the Steward 2.3 m acquisition and guidance TV during the spectroscopic observation.

1E 1549.8+2022: Although in the IPC this source is extended, the HRI observation reveals that the large majority of the IPC X-ray flux is unresolved and coincident with the AGN (see also § III).

3.6 m spectrograph. The red sensitive detectors on these spectrographs have similar spectral ranges of λλ4000–7000 and 10–12 Å resolution across that range. In many cases spectra blueward of 4000 Å were needed to confirm identifications (e.g., to look for the presence of Ca II H and K absorption in weak-lined stars which appear featureless in the lower resolution red spectra). These blue spectra were obtained with a Reticon detector operating in a photon counting mode behind a blue sensitive image tube on the Steward 2.3 m and have 7 Å resolution in the range λλ3400–6000.

Often we were drawn to observe quite faint optical candidates due to their blue color on the POSS or to their positional coincidence with a VLA radio source. All sources estimated to be extragalactic from the f_x/f_v ratio for candidates in the error circle and with $\delta \geq -20°$ were observed at the VLA (Feigelson, Maccacaro, and Zamorani 1982) with a typical sensitivity level of a few mJy and positional accuracy of $\sim 1''$. In all cases where a VLA radio source was detected in the error circle, its optical counterpart is also the proposed X-ray source identification. About one-third of the X-ray sources were detected at 6 cm, making the presence of radio emission an excellent method with which to identify the correct optical counterpart to IPC X-ray sources.

After several sources were already identified, HRI positions became available for about one-third of the sources. In all cases these detections validated our proposed optical counterparts.

With the use of the method of identification described above, the only concern is that in some cases the real X-ray source identification is below the level of the POSS and the object we have identified is present in the error circle by chance, or that more than one plausible counterpart to the X-ray source is present in the error circle. This is unlikely but deserves detailed consideration as follows.

First of all, each of the proposed identifications have the proper f_x/f_v ratio to be the X-ray source based upon previous detections for other members of its optical class. Where the f_x/f_v is somewhat higher than expected, an HRI position confirms the source identifications. For example, normal main-sequence G and K stars are detected at $f_x/f_v = 10^{-6}$ to 10^{-2} (Vaiana *et al.* 1981). In the Medium Survey nine G and K stars are detected with $f_x/f_v = 10^{-4}$ to 10^{-1}. Three stars have a rather high f_x/f_v ratio for their spectral type. For all of them, however, HRI positions confirm the correctness of the identifications (see also § IV*a*). A confirming HRI position is also available for the one anomalous AGN (1E 1207.9+3945) with a two-point spectral slope $\alpha_{ox} = 0.8$ (nominal range $\alpha_{ox} = 0.9$–1.8; Zamorani *et al.* 1981; see Tananbaum *et al.* 1979 for the definition of α_{ox}).

We have further investigated the probability that our proposed identifications are present in the error circle merely by chance and the true identification is fainter than the limit of the POSS. The only classes of objects with a high probability of such a chance superposition are stars and quasars. In the case of the quasars, the faintest proposed optical counterparts listed in Table 1 have $m_v \sim 20.5$. Tyson (1981) estimates that there are ~ 30 quasars per square degree at or above that magnitude. The probability for a quasar to randomly fall in a 60″ radius IPC error circle, therefore, is $\sim 2.5\%$. Thus, of the 31 IPC error circles with $\delta \geq -25°$, we expect $<$ one quasar by chance. Although the number of stars bright enough to be a possible counterpart of the X-ray sources varies considerably with galactic latitude, the mean number for Medium Survey fields is approximately the same as for the quasars, and thus they contribute a similar level of contamination. As an aside, we note that there is already one case (1E 0809.9+4809) for which both a quasar and a bright star are present in the error circle, and, in this case, it is not known which is the X-ray emitter. Therefore, we regard our identifications as quite secure on statistical grounds. It should also be noticed that if we were to investigate X-ray sources a factor of 3–10 fainter than those from the Medium Survey (e.g., those from the Deep Survey) then (*a*) the faintest AGN counterparts would not be visible on the POSS, and (*b*) the enhanced contamination levels, especially from stars, would require higher positional accuracy than provided by the IPC in order to make reliable identifications.

Further support to the identification process comes from the analysis of the angular extent of the X-ray emission. The detection of extended X-ray emission would, in fact, imply the presence of diffuse gas and strongly support a cluster identification while a pointlike X-ray source suggests that a single object is responsible for the X-ray emission. Unfortunately, the majority of sources, as expected in a flux limited survey, are detected near the limit and the consequent lack of a high statistical detection makes the analysis of the X-ray surface brightness distribution often inconclusive. In some cases, however, we were able to recognize a source as extended or to set stringent upper limits on its size. In all these cases, the analysis of the X-ray surface brightness distribution supports the proposed identification. The 23 sources for which an HRI detection indicates that the X-ray emission is confined to a few arcseconds are, in fact, all identified with a stellar object (AGN, BL Lac, star) or the nuclear region of a galaxy. Of the five "IPC only" detections for which the high number of counts allows a meaningful analysis of the extension, four show evidence of extended emission while one does not. The four extended sources are, in fact, identified with clusters of galaxies, while the proposed identification for the unresolved source is a SAO star. However, there are two interesting intermediate cases which require additional discussion.

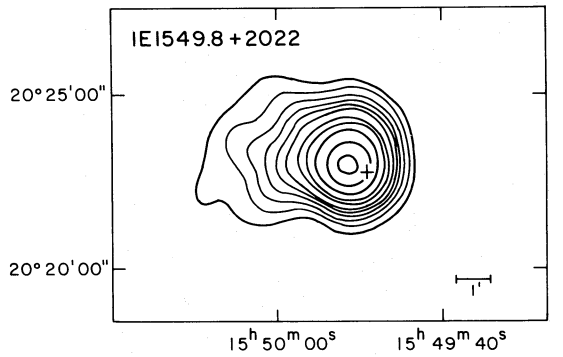

FIG. 2.—Isointensity X-ray contours for the source 1E 1549.8 +2022. Contours have been obtained by smoothing the raw image with a 32″ Gaussian. The + sign marks the position of the AGN responsible for the bulk of the emission. The excess of X-ray emission to the east is probably due to a foreground group of galaxies.

In one case (1E 1549.8+2022) the X-ray emission clearly shows the presence of an unresolved source *plus* some diffuse emission (see Fig. 2). The unresolved component which dominates the X-ray emission is associated with an AGN ($z = 0.250$), as indicated by an HRI image. The faint diffuse component is probably associated with a foreground group of galaxies ($z = 0.135$).

The second case, 1E 0126.4+0725, is identified with the cluster of galaxies Shahbazian 41. We have called Sh 41 a "cluster" even though it consists only of two large galaxies ($M_v \sim -19$) plus numerous compact companions. The limited statistics on the detection of this source prevent a meaningful analysis of the X-ray surface brightness distribution, and we are left with the possibility that the X-ray emission originates in the nuclear region of one of the galaxies, which is also a radio source. In this case, this object would be a further example of an optically "dull", X-ray luminous galaxy (cf. Elvis *et al.* 1981).

In conclusion, we present Figure 3 as a guide for *Einstein Observatory* investigators with unidentified "serendipitous" detections present in their observations. This plot has been constructed for the Medium Survey detections listed in Table 1 and requires only V magnitudes from the POSS (King and Raff 1977) in addition to the X-ray flux. Thus, in areas of the sky where the reprocessed IPC error circle contains only a few optical candidates ($|b^{II}| > 20°$ in general), it should be possible to separate galactic from extragalactic sources, at a high confidence level, without carrying out any new optical observation.

IV. BASIC OPTICAL PROPERTIES OF THE COUNTERPARTS

a) The Stars

Of the X-ray sources in this survey, approximately one-quarter are identified with galactic stars. In Figure 4 we plot as filled circles the logarithm of the X-ray to visual flux ratio, computed in the same way as in Paper I, versus our estimated spectral type for the 15 stellar

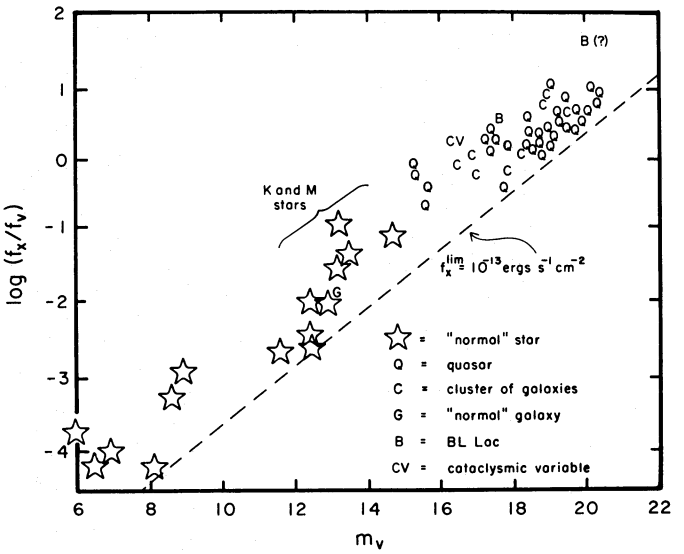

FIG. 3.—Separation of the classes of optical counterparts to the Medium Survey sources based solely upon nonspectroscopic data. Using only the visual magnitudes estimated from the POSS (diameter method of King and Raff 1977) and the X-ray flux, it is possible to separate galactic and extragalactic sources at high confidence level. Only the cataclysmic variable is not distinguishable from the POSS data alone. The galactic-extragalactic dichotomy is further enhanced if crude POSS colors are considered as the faintest stars in this figure are all quite red ($B - V \gtrsim 1.0$) while the brightest quasars are quite blue ($B - V \lesssim 0.4$). The dashed line marks the lowest flux detected in the Medium Survey.

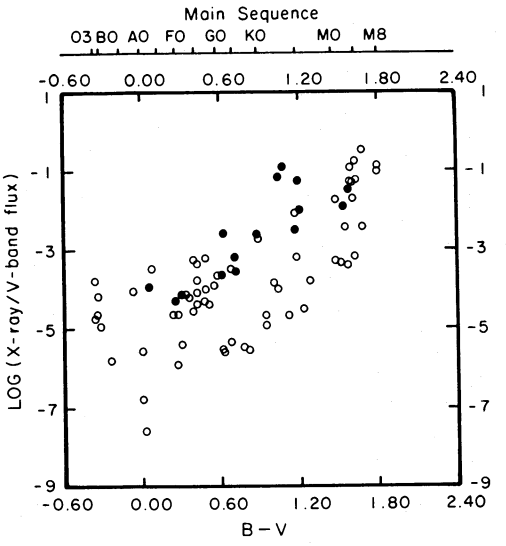

FIG. 4.—Log (f_x/f_v) vs. $B-V$ for the stars detected in the Medium Survey (*filled circles*) compared with the detections from Vaiana *et al.* (1981). Only three stars, all K stars and all with HRI positions, are anomalous when compared to the Vaiana *et al.* detections.

identifications listed in Table 1. These data are compared with the corresponding values (*open circles*) for the dwarf star detections from Vaiana *et al.* (1981). The proposed stellar identifications cover the range from A to middle M and should mostly be dwarfs, although we cannot generally assign a luminosity class at low spectral resolution. All of the Medium Survey stars but one (see § IV*b*) are normal in the sense that their log (f_x/f_v) values are similar to those for stars detected in the pointed *Einstein* observations. Inspection of Figure 4 shows, however, that there are three stars (1E 1339.9+6030, 1E 1548.7+1125, and 1E 1751.0+7046) which have an $f_x/f_v \approx 5-10$ times higher than any of the detections reported by Vaiana *et al.* (1981) for the same spectral range (early to mid-K class). HRI detections are available for all three sources confirming these stars as the X-ray sources. Only in the last object (which has the highest f_x/f_v of the three) is there any evidence for weak Hα emission. Otherwise, there is no indication of any spectral peculiarities which might be related to the enhanced X-ray emission. Due to the relatively low dispersion at which our observations were taken, we could not readily determine whether these stars are RS CVn type binaries, whose more active components are typically G8–K2 (Walter and Bowyer 1981).

b) The Probable Dwarf Nova 1E 1240.8+0312

Many cataclysmic variable (CV) stars have been discovered by X-ray survey satellites, and it was reasonable to suppose that more might have been found at the fainter flux levels reached by the *Einstein Observatory*. However, only one CV candidate was found among the 63 sources of the Medium Survey sample, just as one such object was found in the 40 IPC identifications of Reichert *et al.* (1982).

The source 1E 1240.8+0312 is detected at a fairly high flux level (1.7×10^{-12} ergs cm^{-2} s^{-1}; Table 1). Spectroscopic observations with the Steward 2.3 m reflector on 1981 April 5 showed strong, broad emission lines of hydrogen and neutral helium, as shown in Figure 5. Relative line fluxes and equivalent widths are presented in Table 2; we estimate $V \sim 17.5$ at the time of our observation compared with the measurement from the Palomar Sky Survey (Table 1) of $V \sim 16.5$. When the latter value is used, the X-ray to visual flux ratio for this object ($f_x/f_v = 1.6$) is the highest among the stellar identifications and is significantly higher than the mean for CVs in general (Córdova, Mason, and Nelson 1981). However, since it is not surprising for a CV to vary in optical flux by orders of magnitude, it is of limited value to discuss f_x/f_v when these quantities are obtained at different times. Still, our very high apparent value of f_x/f_v may be a clue to the type of CV that this object is, as we discuss below.

The spectrum shown in Figure 5 is most suggestive of a dwarf nova system. Classical novae generally show strong He II and high excitation emission features. Furthermore, old novae are relatively luminous in quiescence ($M_v = +4$ to $+2$), implying that the system would be at least 1 kpc distant, or at least two disk scale heights out of the Milky Way plane. Since old novae generally show a concentration to the plane, it is unlikely that 1E 1240.8+0312 is one. Similarly, we think it very unlikely that this object is a magnetic AM Her system, despite the large f_x/f_v generally found for these objects and their predilection for being X-ray dis-

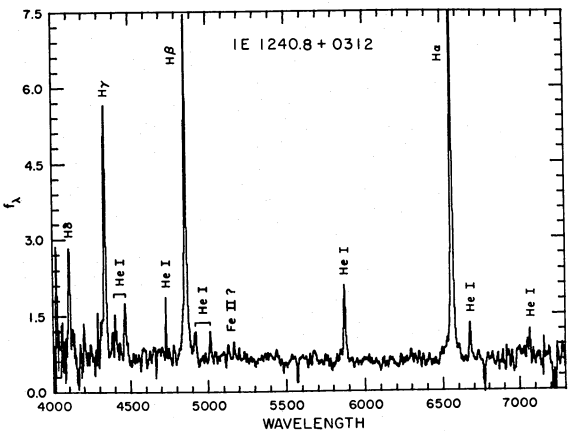

FIG. 5.—A 10 Å resolution spectrum of the cataclysmic variable 1E 1240.8+0312 taken with the Steward 2.3 m telescope on the night of 1981 April 5. Relative line fluxes derived from this spectrum are listed in Table 2.

TABLE 2

EMISSION LINE STRENGTHS FOR 1E 1240.8+0312[a]

Feature	Eq. Width (Å)	Relative Flux	Notes
He I λ4026	18.3	10.3	
Hδ	41.4	22.9	Another feature on red wing
Hγ	91	44.5	
He I λ4388	72	3.4:	
He I λ4471	21	7.9	
He II λ4686	< 2	< 0.5	
He I λ4713	4.7	1.71	
Hβ	151	54.3	
He I λ4921	8	2.9:	On wing of Hβ
He I λ5015	7	2.1:	Including possible Fe II
? ~ λ5130 ?	4	1.3:	
Fe II λ5167 ?	5	1.5:	
He I λ5876	28	8.4	
Hα	264	74.3	
He I λ6678	16	4.8	

[a]Observations made 1981 Apr 5 with the Steward 2.3 m telescope.

covered. Even in their "low" states, AM Her systems show strong He II if the Balmer lines are strong and show nonrecombinational flux ratios.

On the other hand, this emission line spectrum is typical of dwarf novae in quiescence. These are probably also the CV type, most commonly found in optical surveys at high galactic latitude (cf. Green *et al.* 1982), due perhaps to their lower mean luminosities and distances. Furthermore, several dwarf novae have been previously discovered in X-ray surveys, including 1E 0643.0−1648 (Chlebowski, Halpern, and Steiner 1981) and 1E 1551+718 (Mason *et al.* 1982). Dwarf novae systems may vary both their optical and X-ray fluxes by orders of magnitude between quiescence and outburst (e.g. Chlebowski, Halpern, and Steiner, 1981; Córdova, Mason, and Nelson, 1981). Thus, we may speculate that the *Einstein* observation of 1E 1240.8+0312 caught this object in outburst, accounting for the high f_x value relative to our quiescent f_v measurements. The implied outburst magnitude is $V \sim 15$, not unreasonable for a dwarf nova previously unrecorded in the *General Catalogue of Variable Stars*.

c) *The Active Galactic Nuclei*

Thirty-four of the Medium Survey sources (~ 75% of the extragalactic population) are identified with AGNs. The basic properties of these objects are listed in Table 3 where the following information is given:

Col. (i): Source name.

Col. (ii): Redshift.

Col. (iii): The absolute visual magnitude corrected for reddening in our Galaxy.

Co. (iv): Logarithm of the 0.3–3.5 keV X-ray luminosity (ergs s^{-1}) in the source frame.

Col. (v): α_{ox}, the two-point optical-to-X-ray spectral index as defined in Tananbaum *et al.* (1979).

Col. (vi): The spectral type of the AGN in the sense of Weedman (1977) as extended by the Lick group (e.g., Osterbrock 1979). The classifications here are restricted to either type 1, permitted emission lines broader than forbidden lines; type 1.5, permitted emission lines with obvious broad and narrow components present; or type 2, permitted emission lines of approximately equal width to the forbidden lines ($\lesssim 1000$ km s^{-1}). The broad-line component is completely absent or seen only at Hα or Mg II. Thus the Seyfert type 1.9's have been grouped with the Seyfert 2's.

Col. (vii): The observed spectral features including all emission and absorption lines observed. Two of the identifications (1E 1207.9+3945 and 1E 1525.1+1550) are based upon previously published data as referenced in Table 1.

Col. (viii): The Hβ full widths at half-maximum and at zero intensity, in km s^{-1}.

Col. (ix): The flux ratio $f(\mathrm{H}\beta)/f([\mathrm{O\ III}]\ \lambda\lambda 4959, 5007)$.

Col. (x): An *estimated* value for $B-V$ from the spectrophotometry used to make the identifications. This is not accurate photometry because the apertures used were small (2″.5 or 3″.5) and depended on the seeing conditions. Thus, the values quoted here should be used with caution.

Col. (xi): The appearance of the object on the red POSS plate. Where the POSS plates were not available, the plates used for this information are noted.

Col. (xii): comments, particularly in regards to the emission line properties. Where only one emission line was observed, it was always identified as Mg II λ2798 based upon the absence of other strong lines in the wavelength region observed. In these cases the spectral range of the observations is given.

There is one object in Table 3 for which the optical nature is not yet well understood. 1E 1207.9+3945 is an HRI source coincident with a faint ($m_v \sim 20.5$) stellar object 6′ north of NGC 4151. This object was originally discovered at Westerbork in the "background" radio survey of the NGC 4151 field (de Ruiter, Willis, and Arp 1977) and identified by Arp as a quasar with $z = 1.84$. This redshift is based upon two multichannel-scanner observations made with the Hale 5 m telescope; it is derived from weak lines of Mg II, C III], and C IV superposed upon a very red continuum ($\alpha \sim 3$). The continuum may flatten blueward of V band to $\alpha \sim 1$. Also, this object has the smallest α_{ox} in the sample (and thus the highest f_x/f_v). Two spectra obtained by us with the Steward 2.3 m and with the MMT, respectively, do *not* reveal any emission or absorption lines even though

1983ApJ...273..458S

TABLE 3

X-RAY SOURCES IDENTIFIED AS AGNs

(i)	(ii)	(iii)	(iv)	(v)	(vi)	(vii)	(viii)	(ix)	(x)	(xi)	(xii)
SOURCE	z	M_V	log L_X	α_{ox}	SPECTRAL TYPE	OBSERVED SPECTRAL FEATURES	Hβ FWHM/FWZI	Hβ/[OIII]	B-V	POSS APPEARANCE	COMMENTS
1E0111.9-0132	.120	-20.4	43.41	1.17	1.5	Hβ, Hγ, Hδ, [OIII] +[OIII] λ4363	1150/3300	1.0	0.7	FUZZY	
1E0112.9-0147	.284	-21.8	43.75	1.26	2	Hβ, [OIII], [OII], CaII H & K, G band Mg 'b'in absorption	<750/<750	0.5	1.3	STELLAR	
1E0135.0+0339	.637	-25.0	44.76	1.36	1	MgII, [NeV]			0.3	STELLAR	
1E0136.3+0605	.450	-24.3	44.39	1.39	1	MgII, Hβ, Hγ, [OIII], [OII]	6200/13000	4.1	0.2	STELLAR	
1E0144.1-0055	.080	-23.1	43.37	1.60	1.5	Hα, Hβ, Hγ, Hδ, Hε, [OIII], [NeIII] λ3869	1100/5300	1.2	0.7	GALAXY	
1E0412.4-0803	.037	-21.7	43.13	1.47	1.5	Hα, Hβ, Hγ, [OIII] HeII λ4686	780/10000	0.2	0.8	STELLAR	
1E0420.9-3903	.269	-22.5	43.86	1.31	1	Hβ, [OIII], [OII]	6000/12000	5.2	0.7	STELLAR on ESO BLUE	
1E0438.6-1049	.868	-24.5	45.34	1.03	1	MgII, [OII] Possible [NeV]			0.5	STELLAR	
1E0440.0-1057	.279	-22.9	44.00	1.33	1.5	Hβ, Hγ, Hδ, [OIII]	1200/7800	7.4	0.2	STELLAR	
1E0447.1-0917	.946	-26.5	45.13	1.41	1	MgII only			0.1	STELLAR	Spectral coverage: λλ3900-7100 Å
1E0449.4-1823	.338	-23.7	44.66	1.19	2	Hβ, Hγ, Hδ, MgII [OIII] [OIII], [NeV], [NeIII]	630/1200	1.0	0.5	STELLAR	See Stocke et al. (1982a)
1E0450.3-1817	.059	-20.3	42.82	1.34	1.5	Hα, Hβ, Hγ, [OIII], [OII], OI λ6300	<250/18000	2.0	0.9	STELLAR	
1E0809.8+4809	.459	-23.9	44.50	1.31	1	MgII, Hβ, Hγ, Hδ, [OIII]			0.2	STELLAR	Spectrum too noisy near Hβ-OIII to determine line widths and fluxes
1E0838.6+1324	.723	-24.6	44.76	1.29	1	MgII only			0.4	STELLAR	Spectral coverage: λλ4000-7200 Å
1E0849.0+2845	1.273	-25.3	45.29	1.19	1	CIII], MgII			0.5	STELLAR	
1E0849.2+2829	.209	-20.5	43.61	1.10	1	Hβ, Hγ, Hδ, [OIII] [OII]	1500/4800	2.5	0.9	FUZZY	cols. 8 and 9 poorly determined

TABLE 3—*Continued*

(i) SOURCE	(ii) z	(iii) M_V	(iv) log L_x	(v) α_{ox}	(vi) SPECTRAL TYPE	(vii) OBSERVED SPECTRAL FEATURES	(viii) Hβ FWHM/FWZI	(ix) Hβ/[OIII]	(x) B-V	(xi) POSS APPEARANCE	(xii) COMMENTS
1E0849.8+2829	.197	-22.5	43.59	1.41	1	Hβ, Hγ, Hδ, [OIII]	6300/14000	1.9	0.3	STELLAR	
1E0850.0+2828	1.273	-25.8	45.24	1.29	1	CIII], MgII			0.5	STELLAR	
1E0850.2+2825	.922	-27.1	44.86	1.61	1	MgII, [NeV]			0.4	STELLAR	
1E0937.8+1153	.783	-25.7	44.98	1.37	1	MgII only			0.4	STELLAR	Spectral coverage: λλ4000-6000 Å
1E1207.9+3945	1.84?	-26.5?	46.68?	0.85	1 or BL Lac	CIV, CIII], MgII?			0.4	STELLAR	spectrum from H. Arp (de Ruiter, Willis, Arp, 1977) See text
1E1223.5+2552	.067	-21.0	43.17	1.34	1.5	Hα, Hβ, Hγ, Hδ, [OIII]	1000/8000	3.1	0.6	FUZZY	
1E1327.4+3208	.090	-21.6	43.55	1.30	1	Hα, Hβ, Hγ, [OIII], [OII]	5800/8100	2.0	0.6	GALAXY	
1E1415.0+2513	1.057	-24.6	45.19	1.12	1	MgII, probable CIII]			0.5	STELLAR	
1E1415.1+2527	.560	-23.4	44.50	1.20	1	MgII, Hγ, [OII], [NeV]			0.1	STELLAR	
1E1416.7+2524	.674	-25.2	44.65	1.42	1	MgII only			0.5	STELLAR	spectral coverage: λλ4400-6400 Å
1E1525.1+1550	.230	-23.8	44.46	1.28	1	Hβ, Hγ, [OIII]	9500/11000	6.5	0.2	STELLAR	see Grindlay et al. (1980) for spectrum
1E1533.5+1440	.021	-19.9	42.09	1.59	1.5	Hα, Hβ, Hδ, [OIII]	1300/2700	0.5	0.9	GALAXY	
1E1549.8+2022	.250	-24.0	44.70	1.21	1	Hβ, Hγ, Hδ, Hε, [OIII], [OII]	1700/10000	6.7	0.0	STELLAR	
1E1617.9+1731	.116	-24.2	44.10	1.48	1	Hα, Hβ, Hγ, Hδ, He, [OIII]	6000/19000	9.7	0.4	STELLAR	
1E1745.2+2747	.156	-21.8	43.51	1.33	1	Hβ, Hγ, Hδ, [OIII]	6000/12500	1.4	-	STELLAR	
1E2141.6+0400	.410	-23.5	44.43	1.25	1	Hβ, Hγ, [OIII], [OII] [NeV], MgII	4000/9000	2.2	0.3	STELLAR	
1E2204.0-4059	.231	-21.4	44.50	.89	2	Hβ, [OIII]	<1000/<2000	0.1	1.1	STELLAR ON ESO BLUE	
1E2223.6-0517	1.866	-28.3	45.83	1.45	1	C IV, C III]			0.3	STELLAR	

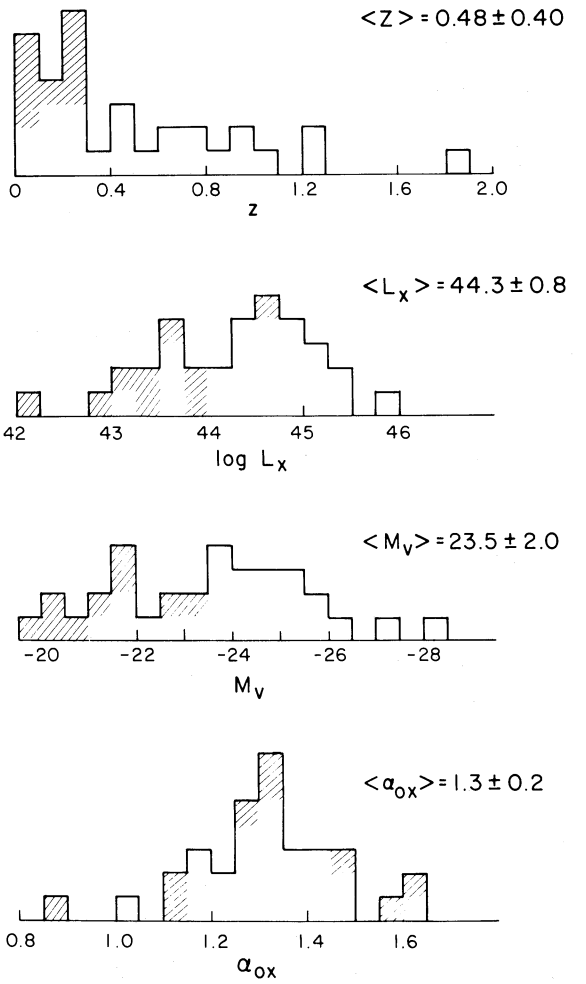

FIG. 6.—The distributions of redshift, X-ray luminosity, absolute magnitude, and two-point optical-to-X-ray spectral index α_{ox} for the AGN sample. The crosshatched objects are the red and marginally red quasars discussed in the text. 1E 1207.9+3945 is not included in this figure due to the uncertainty of its identification (see § IV*c*).

the region of the proposed C III] and C IV line positions were covered by both spectra. We conclude either that the object has recently flared blanketing the lines or that the original identification was incorrect. This object is a possible BL Lacertae candidate given its high f_x/f_v, point radio source coincidence, and steep power law continuum. Further observations are required to clarify the nature of this object.

The redshift, X-ray and optical luminosities, and α_{ox} distributions for our sample of AGNs are shown in Figure 6. These distributions show that high redshift high luminosity quasars are indeed lacking in X-ray selected samples with limiting flux of $\sim 10^{-13}$ ergs cm^{-2} s^{-1} (0.3–3.5 keV), as suggested by other authors (Margon, Chanan, and Downes 1982 and, more recently, Kriss and Canizares 1982 and Reichert *et al.* 1982). The major difference between the present data set and that of Margon, Chanan, and Downes (1982) is that the latter sample contains only AGNs with $m_v \leq 18.5$. Thus, the redshift and luminosity distributions do not seem to be strongly dependent on the limiting optical magnitude to which an X-ray sample is identified, despite the fact that our sample includes what may be a new type of AGN not reported by Margon, Chanan, and Downes (1982) (see § IV*d*).

The "apparent" anomaly of the redshift and optical luminosity distribution of X-ray selected quasars can be explained (see Zamorani 1982 and Maccacaro and Gioia 1983) by the dependence of the X-ray to optical luminosity ratio (L_x/L_o) on L_o and z first suggested by Zamorani *et al.* (1981) and further established by Zamorani (1982) and Avni and Tananbaum (1982).

A recent analysis of the sample of AGNs discussed in this paper has shown that a positive amount of cosmological evolution is required to explain the X-ray data and that the amount of evolution implied by the X-ray data is smaller than the amount derived from the analysis of optically selected samples (Maccacaro *et al.* 1983). Also this difference can be explained by the fact that L_x/L_o is a function of L_o and z (Avni and Tananbaum 1982). Although there is evidence that the framework used to link the redshift distribution and the evolutionary rate of optical and X-ray selected AGNs may be too simple since it also leads to some inconsistencies with the observational data (see Maccacaro *et al.* 1983 for a discussion of the luminosity function), we can safely say that no basic difference in the properties of X-ray selected and optically selected quasars is yet needed to explain the observations.

d) *Red X-Ray Selected AGNs*

There is in our sample a class of objects which has not been clearly identified in other samples of X-ray selected AGNs (although such objects are present in the Reichert *et al.* 1982 survey). These are AGNs with rather reddish colors (six with $B - V > 0.8$; four with $0.6 \leq B - V \leq 0.8$) and spectra which have prominent narrow line components (types 1.5 or 2). The 10 sources in the Medium Survey AGN sample which meet this description are shown as crosshatched boxes in Figure 6. The two red AGNs with the lowest redshifts are clearly galaxies and thus strongly resemble the Seyfert 2 galaxies NGC 5506 (= 3U 1410−03; Bahcall *et al.* 1975), NGC 7582 and NGC 2992 (2A sources; Ward *et al.* 1978), which are low-luminosity (10^{42}–10^{43} ergs s^{-1}) X-ray sources found by the early all-sky surveys. However, the remaining eight are either stellar or slightly fuzzy on the POSS and have substantially higher X-ray luminosities than the Seyfert 2s mentioned above. The prototype for this class is the "narrow-line quasar," 1E 0449.4−1823, which has been previously discussed in some detail by Stocke *et al.*

(1982*a*). This object resembles a high luminosity Seyfert 2 galaxy with strong forbidden lines of [O III], [O II], [Ne III], and [Ne V] and relatively weak Balmer lines on top of a rather reddish continuum ($U-B \approx -0.4$). The lower resolution spectrum of 1E 0449.4−1823 is shown in Figure 7. The broad line component to the permitted lines has now been detected only in Mg II λ2798, but this emission line is still dominated by a strong narrow-line component (see Fig. 8). The width of the line observed at λ3750 in this quasar (FWHM = 2000 km s^{-1}) is consistent with the expected combined widths of the Mg II doublet (λλ2795.5, 2802.7) each broadened by the same amount as Hβ (FWHM = 600 km s^{-1}; Stock *et al.* 1982*a*). Clearly this Mg II profile is very different from those found in almost all quasars; as are the rather weak Mg II lines found in *IUE* spectra of low redshift Seyfert 2 galaxies (Boksenberg *et al.* 1978; Bergeron, Maccacaro, and Perola 1981), in the spectra of red 3CR quasars studied by Smith and Spinrad (1980) and in the spectra of some radio galaxies (e.g. 3C 234; Grandi and Osterbrock 1978). Thus at higher redshift, objects similar to this one would likely still be distinct from most quasars. We also note that if the broad base is, in fact, due to Mg II emission, then reddening is clearly excluded as the mechanism eliminating the broad component at Hβ (see Fig. 7) in this QSO. However, we cannot exclude the possibility that the broad base in Figure 8 is largely due to Fe II emission particularly since the blue wing appears stronger (see Grandi 1981).

Bearing in mind that the $B-V$ colors for the AGNs listed in Table 3 must be used with extreme caution (see § IV*c*), we have estimated $U-B$ colors assuming that the continuum can be best fit with a single power law (Matthews and Sandage 1963). This seems to be a reasonable assumption based upon the limited wavelength coverage of our spectra (λλ4000–7000) for all objects except 1E 0112.9−0147 where stellar absorption is very clearly seen and the colors are those of a redshifted normal galaxy. In this case, the quoted $B-V$ is typical of a normal early-type galaxy (see notes to Table 1). We have some evidence that the color values derived are not dominated by the necessary use of small entrance apertures for good spectral resolution because several objects were reobserved at different zenith angles, and the results agree within ±0.2 in $B-V$. Also, as noted below, there is a very strong correlation between the objects with reddish colors and those which show an absence of a dominant broad-line component at Hβ. Since Seyfert 2 galaxies are known to be systematically redder than Seyfert 1 galaxies (Weedman 1977), this correlation is expected and further supports the validity of our color estimates.

Six of the 10 crosshatched objects in Figure 6 have estimated $U-B$ much too red ($U-B \geq -0.3$) to be found in UV excess surveys (e.g., Braccesi *et al.* 1980; Schmidt and Green 1983). The spectra of three of these 10 objects show only narrow Hβ lines; four have composite Hβ lines with broad and narrow components of comparable equivalent widths; and two of the three remaining objects have Hβ lines with FWHM values only slightly broader (FWHM ~ 1100 km s^{-1}) than the widths of the forbidden lines. Therefore the red (low redshift, X-ray selected) quasars are also those with relatively weak permitted lines compared to most quasars. In only one case (1E 0112.9−0147) is there clear evidence that the redder continuum is due to starlight, and thus the majority of these quasars are red due to an intrinsically redder power-law continuum.

Since these reddish AGNs would not be found by standard color techniques, they would also not be accounted for in estimates of quasar space densities (e.g., Schmidt and Green 1983). As a consequence, estimates of the quasar contribution to the X-ray background based on optical counts will neglect the contributions from this class of objects.

Figure 7 is a collage of spectra illustrating the variation in Hβ line widths, strengths, and profiles found among the Medium Survey AGNs and is presented to emphasize the wide variety of spectra found. Although accurate photometry is very much needed to confirm this result, note the gradual shift in color from the typical broad-line objects (e.g., 1E 1549.8+2022) to the reddish narrow-line objects (e.g., 1E 2204.0−4059 and 1E 1533.5+1440). Clearly the latter group of objects is very different from the typical optically selected quasars whose permitted emission lines are several thousand km s^{-1} wide (Strittmatter and Williams 1976) and with no obvious signs of a narrow-line component.

Table 3 shows that the reddish AGNs are on average characterized by the lowest X-ray luminosities in the sample. The same is true for the Seyfert 2 galaxies in the *HEAO 1* A-2 survey (Piccinotti *et al.* 1982). Thus, in most respects, these reddish AGNs may be considered as high luminosity Seyfert 2 galaxies. We note that four Seyfert 2 galaxies (also known as narrow emission-line galaxies) whose X-ray spectra are published (Maccacaro, Perola, and Elvis 1982; Mushotzky 1982) clearly show a low-energy spectral cutoff at ~ 2–3 keV implying a large column density of neutral hydrogen ($\geq 10^{22}$ cm^{-2}) around the X-ray emitting region. Evidence has been presented that the amount of absorption increases with decreasing X-ray luminosity (see Fig. 4 of Lawrence and Elvis 1982). As a consequence, in a sample of AGNs selected in the soft X-ray band, the low luminosity objects will be underrepresented, relative to harder X-ray surveys, with respect to the high luminosity objects ($> 10^{44}$ ergs s^{-1}) at a rate which increases with decreasing X-ray luminosity. A more detailed discussion of this effect and its consequences on the shape of the X-ray luminosity function of AGNs is given in Maccacaro *et al.* (1983).

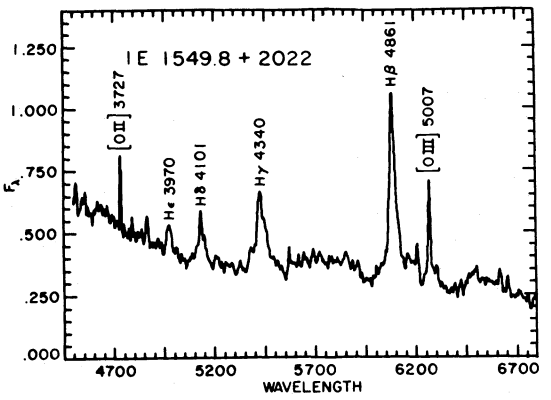

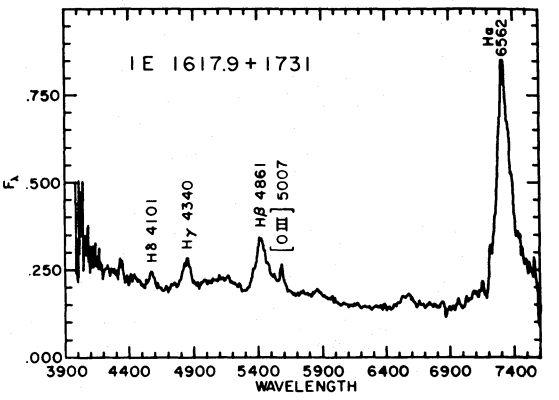

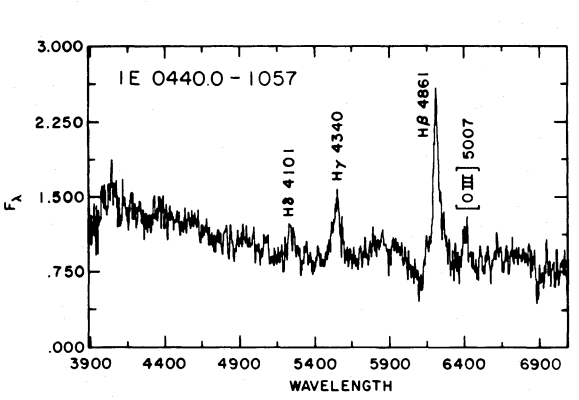

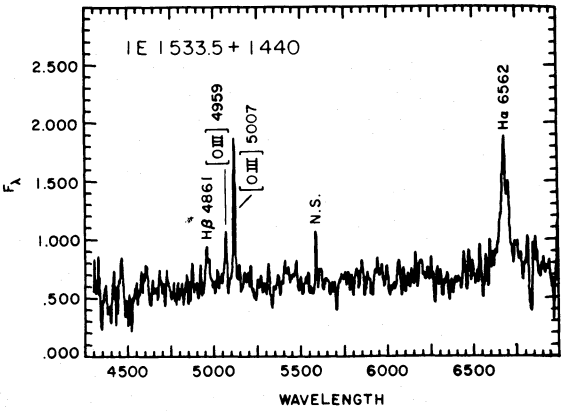

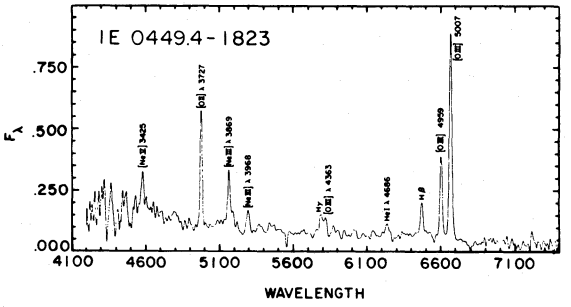

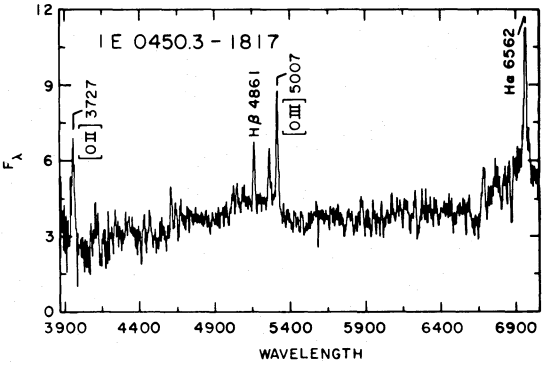

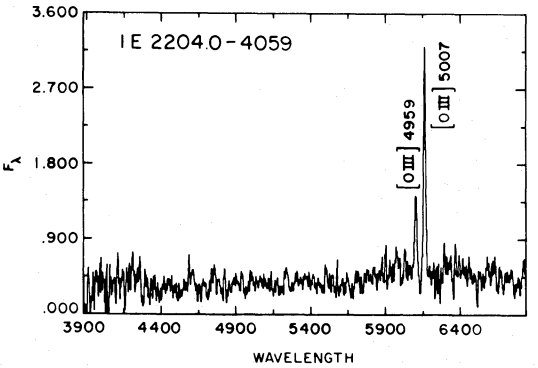

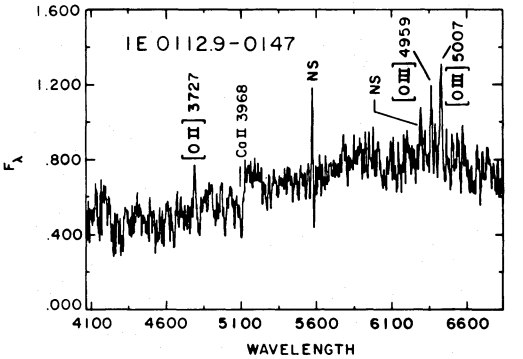

FIG. 7.—Selected spectra of AGNs detected in the Medium Survey. Notice the gradual shift in color from the broad-line "type 1" quasars to the quasars whose spectra contain significant contributions to the permitted line flux from a narrow-line component. The extreme narrow-line object 1E 0112.9−0147 actually shows Ca II H and K absorption and colors typical of a normal galaxy (see notes to Table 1).

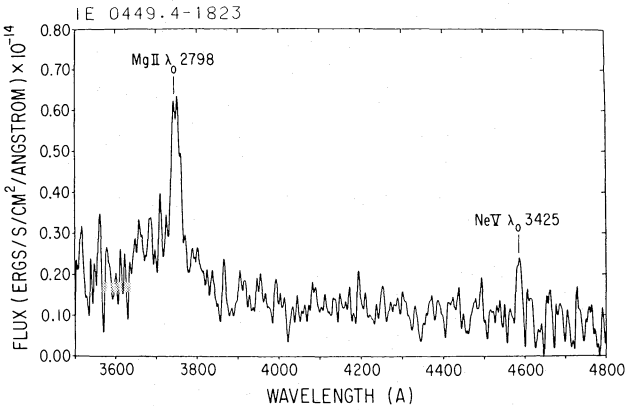

FIG. 8.—A near-ultraviolet spectrum of 1E 0449.4−1823 at 4 Å resolution. The unique Mg II $\lambda_0 2798$ profile has approximately equal contributions from broad and narrow-line components although we cannot exclude the possibility that the broad base is due at least in part to Fe II emission (Grandi 1981).

These reddish AGNs are also helpful in understanding some of the correlations for X-ray emitting AGNs proposed by Kriss, Canizares, and Ricker (1980) where it is suggested that Seyfert 1 and 2 galaxies populate high and low luminosity portions of the same distributions. Figure 9*a* is a plot of the flux ratio Hβ/[O III] versus X-ray luminosity for X-ray selected objects from this paper and from Grindlay *et al.* (1980), plus optically selected Seyferts from Kriss, Canizares, and Ricker (1980) and optically selected quasars from Yee (1980) for which X-ray detections were made with the *Einstein Observatory* (Zamorani *et al.* 1981; Ku, Helfand, and Lucy 1980). The X-ray luminosity of 3C 232 is from E. Feigelson (1982, private communication). We have not plotted the Seyfert 2 galaxies in Kriss, Canizares, and Ricker (1980) for which only X-ray upper limits are available as they generally have $L_x < 10^{42}$ ergs s^{-1}. If we restrict the discussion to broad-line objects only, no correlation or only a very weak correlation is present in the data (see Grindlay *et al.* 1980, Reichert *et al.* 1982, and Kriss and Canizares 1982 for a more detailed discussion of this point). The few high-luminosity X-ray emitting narrow-line AGNs which have been discovered appear to scatter below the broad-line objects over a large range in X-ray luminosity. However, they are too sparse in number to convincingly show the existence of a second sequence of narrow-line objects below the broad-line correlation. Such a dichotomy is evident in the larger homogeneous data set of Yee (1980) shown in Figure 9*b* as a plot of the Hβ/[O III] flux ratio versus the nonthermal optical luminosity (since L_x roughly scales as L_{NT}; Kriss, Canizares, and Ricker 1980; Zamorani *et al.* 1981). Much of the scatter in this figure at low nonthermal luminosities is undoubtedly due to the difficulty in estimating the nonthermal fraction in a continuum dominated by starlight. These two sequences become even more evident if the Hβ/[O III] flux ratio is compared to $L_{H\beta}$ since $L_{H\beta} \propto L_{NT}$ and does not suffer from the difficulty with L_{NT} described above (H. Yee 1982, private communication). Nevertheless, the two sequences of broad- and narrow-line objects are clearly visible in Figure 9, and it is clear that the Seyfert 1 and 2 galaxies are not part of the same correlation contrary to the suggestion by Kriss, Canizares, and Ricker (1980). Despite the indication that there are two separate classes of AGNs present in Figure 9, we nonetheless agree with Downes *et al.* (1981) that the spread in this luminosity indicator even within each class is too great to become a useful cosmological test.

A similar analysis of the proposed correlation of FWZI of Hβ with L_x (Kriss, Canizares, and Ricker 1980) also clearly shows that the Seyfert 1 and 2 galaxies comprise two separate sequences (as would be expected since the line widths in question are formed in physically distinct regions). The remaining correlation between FWZI (Hβ) and L_x for the broad-line objects alone is, at best, extremely weak.

In summary, the AGNs found in the *Einstein Observatory* Medium Sensitivity Survey are primarily low-redshift and low-luminosity objects with distributions similar to those found in other samples (Margon, Chanan and Downes 1982; Kriss and Canizares 1982; Reichert *et al.* 1982). However, a sizable fraction of the AGN sample consists of reddish objects ($B - V > 0.6$) whose spectra show prominent narrow-line components to the Balmer lines. We note that these objects have been discovered by virtue of their X-ray emission and that they may represent a separate sequence of AGNs accounting for a substantial fraction, ~25%, of the low-luminosity population.

e) The 0849+28 Field: Quasar Pairs

We would like to draw particular attention to one IPC field centered at $\alpha = 08^h49^m37^s$, $\delta = +28°31'00''$ to observe the bright star HD 75732. This field contains five serendipitous sources which satisfy the criteria to be included in the Medium Survey (see Paper I). All of them are identified with AGNs. Four of these objects constitute two pairs of quasars with very similar redshifts (see Table 4). In a recent paper, Oort, Arp, and de Ruiter (1981) have identified 12 such pairs and have interpreted their physical separation on the sky (10–60 Mpc; $H_0 = 50$ km s^{-1} Mpc^{-1}) and low-velocity differences ($\Delta z < 0.003$) as evidence that these quasars are members of the same supercluster. Margon, Chanan, and Downes (1981) have also identified a serendipitous X-ray source 8′ from 3C 345 as a quasar with redshift identical to that of 3C 345 (± 0.001) but physically distinct from it. The inferred separation for this pair is ~10 Mpc ($H_0 = 50$ km s^{-1} Mpc^{-1}) so these two ob-

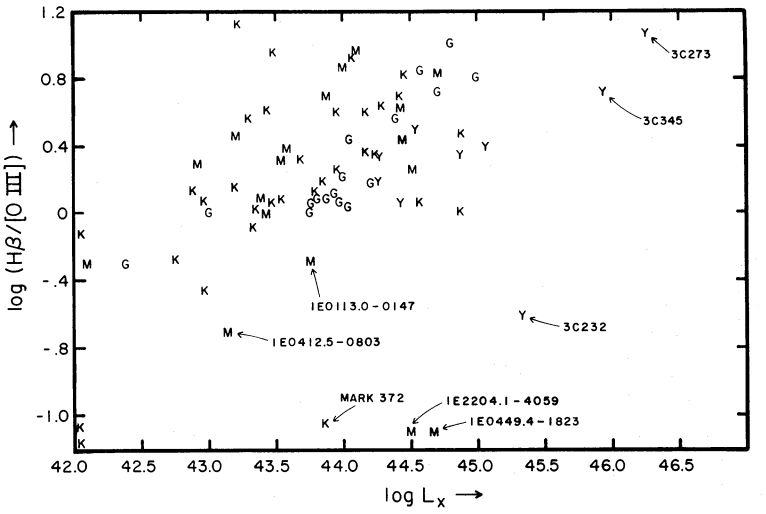

FIG. 9*a*

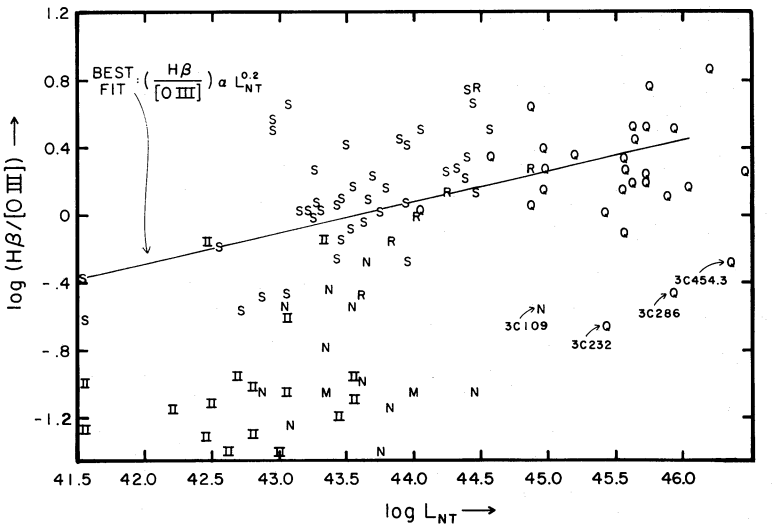

FIG. 9*b*

FIG. 9.—(*a*) The flux ratio of Hβ to [O III] vs. the X-ray luminosity for both X-ray and optically selected objects. Objects include Seyferts and quasars from this paper (M), from Kriss, Canizares, and Ricker (1980) (K), from Grindlay *et al.* (1980) (G), and from Yee (1980) (Y). The X-ray observation of 3C 232 was provided by E. Feigelson (1982, private communication). (*b*) The flux ratio of Hβ to [O III] versus the optical nonthermal luminosity from Yee (1980). The symbols describe the type of object plotted: quasar (Q), Seyfert type 1 (S), Seyfert type 2 (II), broad-line radio galaxy (R), and narrow-line galaxy (N). Also plotted are approximate positions for the two most luminous narrow-line objects in the Medium Survey (M) using approximate L_{NT} values assuming negligible contribution from starlight. Note the two sequences of objects with approximately equal slopes in this diagram.

jects are an additional candidate for quasar pairs in a supercluster.

Using the very simplified arguments of Oort, Arp, and de Ruiter, the high redshift pair in Table 4 has a low probability (< 6%) to be a chance coincidence. The occurrence of this pair seems even more unlikely *a posteriori*, since these two quasars have redshifts so much higher than the bulk of the sample that their coincidence in redshift is even more unusual. This pair has the correct physical separation on the sky to be members of the same supercluster. They are certainly physically distinct quasars (i.e., not a gravitational splitting of the same image) because one is a strong radio source and the other is not (Feigelson, Maccacaro, and Zamorani 1982). The Δz of the low redshift pair is large enough that its chance occurrence is nonnegligible (~ 30%). Moreover, the velocity difference is much too large to be due to the presence of a rich cluster gravita-

TABLE 4

PAIRS OF QUASARS IN THE 0849+28 IPC FIELD

Source	z	m_v	$S_{6\,cm}$	Projected Physical Separation	Δv
1E 0849.0+2845 ...	1.273 ± 0.003	20.5	336 mJy	8 Mpc	< 800 km s^{-1}
1E 0850.0+2828 ...	1.273 ± 0.003	20.0	< 1.9 mJy		
1E 0849.2+2829 ...	0.209 ± 0.002	20.5	< 1.5 mJy	1.6 Mpc	3000 km s^{-1} (35 Mpc)
1E 0849.8+2820 ...	0.197 ± 0.003	18.5	< 1.4 mJy		

tional potential. Thus, given the large physical separation of this pair inferred from its velocity difference, we conclude that the two low redshift quasars are not physically related.

It is surprising that the Medium Survey has already discovered one pair of physically related quasars because the number of sources identified per field is small. Moreover, at the average redshift of our sample ($z \sim 0.5$) the dimension of a supercluster is estimated to be $\sim 3°$, based upon a 40 Mpc size typical of local superclusters (Oort, Arp, and de Ruiter 1981). With only a 32×32 arcmin^2 field of view to sample the sky (the area inside the "ribs" of the IPC), it is indeed surprising that one such pair has already been discovered. This leads us to suggest that an all-sky X-ray survey as sensitive as the Medium Survey will discover large numbers of quasar pairs. The positions and redshifts of these quasars will allow us to map the distribution of matter out to $z \sim 1$ in the same manner that luminous O and B stars allowed us to map the galactic spiral structure. Such an all-sky survey is scheduled for the German satellite *ROSAT* (Trumper 1982).

f) *The Clusters of Galaxies*

Eight X-ray sources are identified with groups or clusters of galaxies (see Table 5), somewhat less than the expected number (12) in the Medium Survey derived from the *HEAO 1* A-2 cluster luminosity function (Piccinotti *et al.* 1982). The eight in Table 5 include Shahbazian 41 (1E 0126.4+0725) despite reservations about the nature of this X-ray source as discussed in § II. As can be seen from the finding charts, the five detections with $z < 0.2$ are best described as poor clusters or compact groups of galaxies. The richest nearby grouping detected in this survey is Abell 744 (1E 0904.5 +1650), a richness class 0 cluster. The other three clusters are too distant to properly evaluate their richness using POSS data alone. An attempt to measure the central galaxy density of the five nearby groups in the manner of Bahcall (1977) yields $\bar{N}_0 \lesssim 20$. Based upon the weak but apparently real correlation between $\bar{N}_0$ and the temperature of the X-ray emitting gas found for richer clusters by Smith, Mushotzky, and Serlemitsos

TABLE 5

GROUPS AND CLUSTERS OF GALAXIES DETECTED IN THE MEDIUM SURVEY

Source Position	f_x (0.3–3.5 keV) $\times 10^{-13}$ ergs s^{-1} cm^{-2}	z	Estimated L_x (2–10 keV) $\times 10^{44}$ ergs s^{-1}
1E 0126.4+0725	4.8	0.085	0.8
1E 0439.3−1102	2.3	0.152	3.2
1E 0904.5+1650	8.7	0.074	2.8
1E 1201.5+2823	8.0	0.167	12
1E 1208.7+3928	2.6	0.34	15
1E 1416.2+2525	6.9	0.29	36
1E 1454.0+2232	2.3	0.108	1.3
1E 1910.5+6736	8.7	0.246	27

(1979), we conservatively estimate $T_x \lesssim 6$ keV for all objects in Table 5. This is certainly an overestimate of the actual temperature for the nearby clusters and may also be for the more distant clusters if the decrease in T_x with z reported by Perrenod and Henry (1981) for some distant clusters is universal. Each of the 2–10 keV luminosities in Table 5 is calculated based upon properly redshifted T_x values estimated from $\bar{N}_0$. If T_x were as low as 2 keV for these clusters, it would reduce the estimates of L_x by only a factor of $\lesssim 2$. Thus the L_x values are not significantly affected even given the large uncertainty in T_x.

The X-ray luminosities found in the Medium Survey span the range of cluster luminosities detected by *HEAO 1* A-2. In Table 6 we compare the Medium Survey detections with the expected detections based upon the Piccinotti *et al.* (1982) power-law fit to the X-ray luminosity function for *HEAO 1* A-2 clusters [$N(L) = N_0 L^{-2.1}$]. See Maccacaro *et al.* (1982) for the details of this calculation. The numbers of Medium Survey detections are as yet far too few to make detailed comparisons, but we do not yet see a strong deficiency of high X-ray luminosity clusters. Such a deficiency is expected if dynamical evolution effects are strong (e.g., Perrenod 1978). On the other hand, there is a marginal deficiency of low-luminosity clusters which already suggests a flattening in the power-law luminosity function below 10^{44}

TABLE 6

X-RAY CLUSTERS: EXPECTED VERSUS OBSERVED FOR THE MEDIUM SURVEY

Log L_x (2–10 keV)	Expectation	Observed
43.5–44	5	1
44–44.5	3	2
44.5–45	2	1
45–45.5	1	3
45.5–46	0	1

ergs s^{-1}, an effect marginally seen in the *HEAO 1* A-2 data as well (McKee *et al.* 1980).

Although the current size of the Medium Survey prohibits any meaningful comparisons, the enlargement of this sample will eventually allow a detailed statistical study of the evolution of clusters as X-ray sources. It is clear that the X-ray flux levels of this survey detect clusters out to $z = 0.2$–0.3, epochs where the dynamical models of Perrenod (1978) already predict significant differences in the X-ray properties of clusters. An X-ray selected sample also avoids the possible Malmquist bias that may be introduced into the study of cluster evolution by observing optically selected clusters (see Henry *et al.* 1979; White, Silk, and Henry 1981) since optically selected distant clusters are chosen in a subjective way and may represent only the richest, most dynamically evolved clusters at those epochs.

The relatively low percentage (15%) of Medium Survey sources identified with clusters makes it clear that several hundred *Einstein Observatory* sources will have to be identified before a cluster sample large enough for statistical studies can be gathered. But the full *Einstein Observatory* data base easily contains this many "serendipitous" sources and, therefore, the selection of a large statistical sample of X-ray clusters is a high priority for future Medium Survey investigations.

V. CONCLUSIONS

The major conclusions of this paper are:

1. We expect that virtually all X-ray sources in the flux range of the Medium Survey can be identified with objects visible on the POSS. This expectation is based upon the complete identification of all sources north of $-25°$ declination where we had at our disposal: (*a*) the POSS two-color plates and (*b*) VLA radio data (Feigelson, Maccacaro, and Zamorani 1982).

2. The optical identifications have the following percentage breakdown: stars (25%), AGNs (56%), and clusters of galaxies (15%). BL Lac objects and "normal" galaxies account for the remaining 4%. These objects have f_x/f_v values at the high end of the ranges previously found for pointed X-ray detections in each class, as would be expected for an X-ray selected sample.

3. There is no evidence for a significant population of "blank field" X-ray sources at this flux level and thus no evidence for any new class of X-ray source with very high L_x/L_v. This is, of course, quite different from the radio surveys which contain a significant fraction of "blank field" sources regardless of radio flux level.

4. Most of the quasars detected in this survey are spectroscopically similar to optical or radio selected quasars. However, $\sim 25\%$ of the quasar sample have reddish colors and permitted lines dominated by a narrow-line component (FWHM $\lesssim 1000$ km s^{-1}). These objects form a second sequence of AGNs, distinct in their optical properties from the broad-line objects.

5. Due to the large number of sources that will soon be available in the flux range of the Medium Survey from the *Einstein* data banks and the 100% identification rate reachable with present-day telescopes, the flux range of this survey becomes the most effective range in which to investigate the nature of the source counts, as well as the cosmic evolution of the classes of objects associated with these X-ray sources.

We are currently involved in expanding the *Einstein* Medium Sensitivity Survey, first doubling it with complete optical identifications to verify the statistical finding reported here, and then cataloging a much larger number of serendipitous sources primarily to investigate the X-ray source counts.

This work would not have been possible without the support of the Multiple Mirror Telescope Observatory and Steward Observatory staffs. In particular, we note the role played by the photon counting reticon detector projects at CfA (D. Latham and J. Geary) and at Steward (D. Mitchell, R. Cromwell, R. Macklin, D. Rautenkrantz, and others). We would like to thank Drs. J. Grindlay, D. Latham, M. Smith, J. Steiner, and M. Ward for communicating results of optical spectroscopy on objects in several of the X-ray fields. We thank Drs. H. Arp, R. Schild, and E. Feigelson for communicating results prior to publication. We also thank J. Flora and M. Wenz for help in preparing this manuscript for publication.

This work has been primarily funded by NASA grant NAG-8370 and has also received support from NASA contract NAS8-30751 and from the Italian PSN (Piano Spaziale Nazionale).

REFERENCES

Abell, G. 1957, *Ap. J.* (*Supp.*), **3**, 211.
Avni, Y., and Tananbaum, H. 1982, *Ap. J.* (*Letters*), **262**, L17.
Bahcall, J., Bahcall, N., Murray, S., and Schmidt, M. 1975, *Ap. J.* (*Letters*), **199**, L9.

Bahcall, N. 1977, *Ap. J.* (*Letters*), **217**, L77.
Bergeron, J., Maccacaro, T., and Perola, C. 1981, *Astr. Ap.*, **97**, 94.
Boksenberg, A., *et al.* 1978, *Nature*, **275**, 404.
Braccesi, A., Zitelli, V., Bonoli, F., and Formiggini, L. 1980, *Astr. Ap.*, **85**, 180.
Chlebowski, T., Halpern, J., and Steiner, J. 1981, *Ap. J.* (*Letters*), **247**, L35.
Colla, G., *et al.* 1972, *Astr. Ap. Suppl.*, **7**, 1.
Córdova, F., Mason, K., and Nelson, J. 1981, *Ap. J.*, **245**, 609.
de Ruiter, H., Willis, A., and Arp, H. 1977, *Astr. Ap. Suppl.*, **28**, 311.
Downes, R., Chanan, G., Anderson, S., and Margon, B. 1981, *Bull. AAS*, **13**, 799.
Elvis, M., Schreier, E., Tonry, J., Davis, M., and Huchra, J. 1981, *Ap. J.*, **246**, 20.
Feigelson, E., Maccacaro, T., and Zamorani, G. 1982, *Ap. J.*, **255**, 392.
Giacconi, R., *et al.* 1979, *Ap. J.* (*Letters*), **234**, L1.
Gioia, I. M., *et al.* 1983, in preparation.
Grandi, S. 1981, *Ap. J.*, **251**, 451.
Grandi, S., and Osterbrock, D. 1978, *Ap. J.*, **220**, 783.
Green, R., Ferguson, D., Liebert, J., and Schmidt, M. 1982, *Pub. A.S.P.*, **94**, 560.
Griffiths, R. E., *et al.* 1983, *Ap. J.*, **269**, 375.
Grindlay, J., *et al.* 1980, *Ap. J.* (*Letters*), **239**, L43.
Henry, J. P., Branduardi, G., Briel, U., Fabricant, D., Feigelson, E., Murray, S., Soltan, A., and Tananbaum, H. 1979, *Ap. J.* (*Letters*), **234**, L15.
Huchra, J., *et al.* 1983, in preparation.
King, I., and Raff, M. 1977, *Pub. A.S.P.*, **89**, 120.
Kriss, G., and Canizares, C. 1982, *Ap. J.*, **261**, 51.
Kriss, G., Canizares, C., and Ricker, G. 1980, *Ap. J.*, **242**, 492.
Ku, W., Helfand, D., and Lucy, L. 1980, *Nature*, **288**, 323.
Lawrence, A., and Elvis, M. 1982, *Ap. J.*, **256**, 410.
Luyten, W., and Miller, F. 1956, *A Search for Faint Blue Stars*, Vol. **13** (Minneapolis: University of Minnesota Observatory).
Maccacaro, T., Anvi, Y., Gioia, I. M., Giommi, P., Griffiths, R. E., Liebert, J., Stocke, J., and Danziger, J. 1983, *Ap. J.* (*Letters*), **266**, L73.
Maccacaro, T., and Gioia, I. M. 1983, in *IAU Symposium 104, Early Evolution of the Universe and its Present Structure*, ed. G. Abell and G. Chincarini, (Dordrecht: Reidel), in press.
Maccacaro, T., Perola, G. C., and Elvis, M. 1982, *Ap. J.*, **257**, 47.
Maccacaro, T., *et al.* 1982 *Ap. J.*, **253**, 504 (Paper I).
Margon, B., Chanan, G., and Downes, R. 1981, *Nature*, **290**, 480.
_____. 1982, *Ap. J.* (*Letters*), **253**, L7.
Mason, K., Reichert, G., Bowyer, S., and Thorstensen, J. 1982, *Pub. A.S.P.*, **94**, 521.
Matthews, T., and Sandage, A. 1963, *Ap. J.*, **138**, 30.
McKee, J., *et al.* 1980, *Ap. J.*, **242**, 843.
Mushotzky, R. 1982, *Ap. J.*, **256**, 92.
Oort, J., Arp, H., and de Ruiter, H. 1981, *Astr. Ap.*, **95**, 7.
Osterbrock, D. 1979, *A.J.*, **84**, 901.
Perrenod, S. 1978, *Ap. J.*, **226**, 566.
Perrenod, S., and Henry, J. 1981, *Ap. J.* (*Letters*), **247**, L1.
Piccinotti, G., Mushotzky, R. F., Boldt, E. A., Holt, S. S., Marshall, F. E., Serlemitsos, P. J., and Shafer, R. A. 1982, *Ap. J.*, **252**, 485.
Reichert, G. A., Mason, K. O., Thorstensen, J. R., and Bowyer, S. 1982, *Ap. J.*, **260**, 437.
Schmidt, M., and Green, R. 1983, *Ap. J.*, **269**, 352.
Schwartz, D., Madejski, G., and Ku, W. 1982, in *IAU Symposium 97, Extragalactic Radio Sources*, ed. D. Heeschen and C. Wade (Dordrecht: Reidel), p. 383.
Smith, B., Mushotzky, R., and Serlemitsos, P. 1979, *Ap. J.*, **227**, 37.
Smith, H., and Spinrad, H. 1980, *Ap. J.*, **236**, 419.
Stocke, J., Liebert, J., Danziger, J., Lub, J., Maccacaro, T., Griffiths, R., and Giommi, P. 1982*b*, *M.N.R.A.S.*, **200**, 27p.
Stocke, J., Liebert, J., Maccacaro, T., Griffiths, R., and Steiner, J. 1982*a*, *Ap. J.*, **252**, 69.
Steiner, J. E., Grindlay, J. E., and Maccacaro, T. 1982, *Ap. J.*, **259**, 482.
Strittmatter, P. and Williams, R. 1976, *Ann. Rev. Astr. Ap.*, **14**, 307.
Tananbaum, H., *et al.* 1979, *Ap. J.* (*Letters*), **234**, L9.
Trumper, A. 1982, Proc. 14th COSPAR Meeting, Ottawa.
Tyson, J. 1981, *Ap. J.* (*Letters*), **248**, L89.
Vaiana, G., *et al.* 1981, *Ap. J.*, **245**, 163.
Walter, F. M., and Bowyer, S. 1981, *Ap. J.*, **245**, 671.
Ward, M., Wilson, A., Penston, M., Elvis, M., Maccacaro, T. and Tritton, K. 1978, *Ap. J.*, **223**, 788.
Weedman, D. 1977, *Ann. Rev. Astr. Ap.*, **15**, 69.
White, S., Silk, J., and Henry, P. 1981, *Ap. J.* (*Letters*), **251**, L65.
Yee, H. 1980, *Ap. J.*, **241**, 894.
Zamorani, G. 1982, *Ap. J.* (*Letters*), **260**, L31.
Zamorani, G., *et al.* 1981, *Ap. J.*, **245**, 357.

I. J. DANZIGER: European Southern Observatory, 8046 Garching bei Munchen, West Germany

I. M. GIOIA and T. MACCACARO: Harvard-Smithsonian Center for Astrophysics, 60 Garden Street, Cambridge, MA 02138

R. E. GRIFFITHS: Space Telescope Science Institute, 173 Rowland Hall, Homewood Campus, Baltimore, MD 21218

D. KUNTH: Institut d'Astrophysique, 98 bis Bd. Arago, F-75014 Paris, France

J. LIEBERT and J. T. STOCKE: Steward Observatory, University of Arizona, Tucson, AZ 85721

J. LUB: Sterrewacht, Leiden, 2300 RA Léiden, The Netherlands

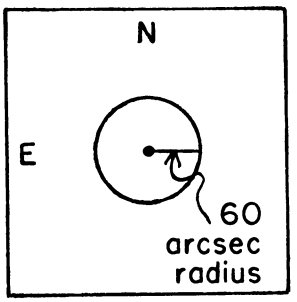

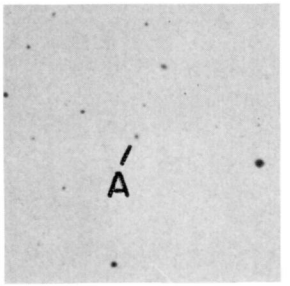

0111.9 - 0132

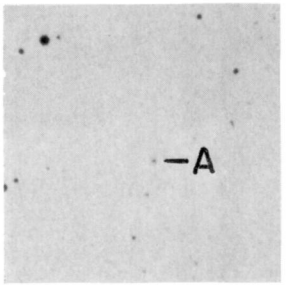

0112.9 - 0147

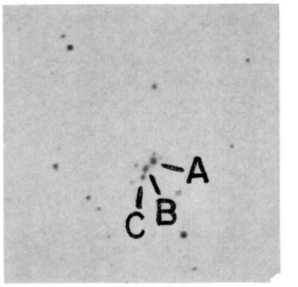

0126.4 + 0725

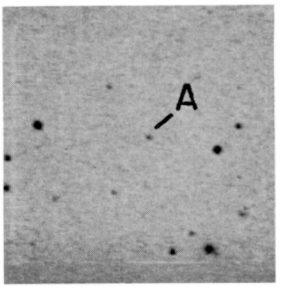

0135.0 + 0339
O PLATE

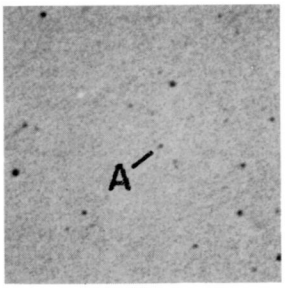

0136.3 + 0605

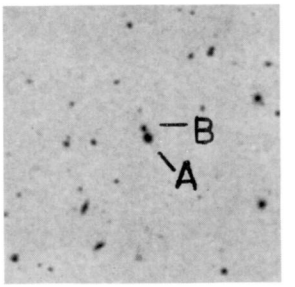

0144.1 - 0055

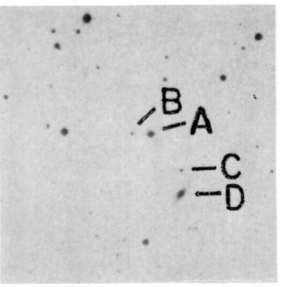

0412.4 - 0803

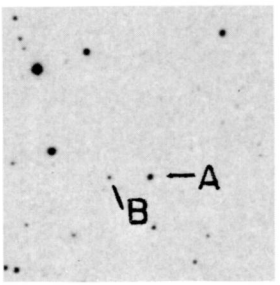

0420.1 - 3838

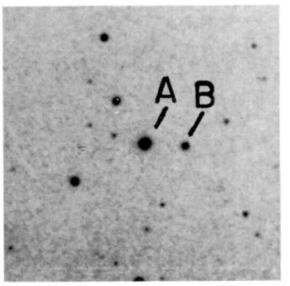

0420.3 - 3859

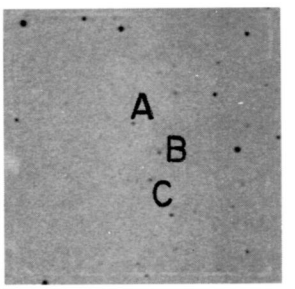

0420.9 - 3903
ESO BLUE

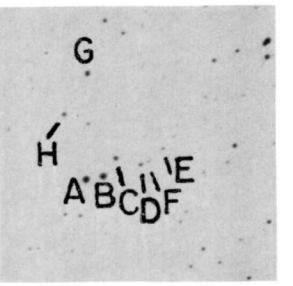

0438.6 - 1049

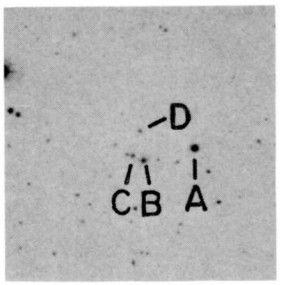

0439.3 - 1102

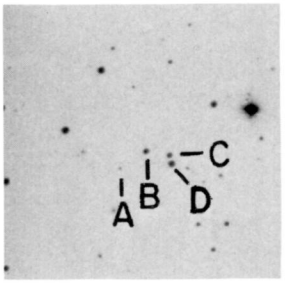

0440.0 - 1057

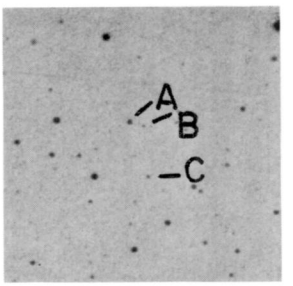

0447.1 - 0917

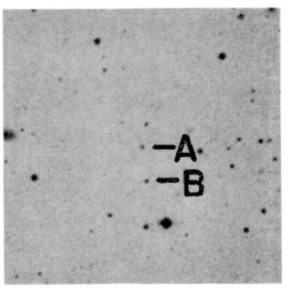

0449.4 - 1823

FIG. 1.—Finding charts for the Medium Survey sources listed in Table 1. All charts are 7× reproductions from the Palomar Observatory Sky Survey red plates or the Whiteoak extension red prints unless otherwise noted. Each chart is centered on the X-ray source centroid. The marked objects were spectroscopically observed and are described in Table 1. The chart for 1E 0622.5−5255 has been artificially enhanced to clearly show the field (obscured by Canopus).

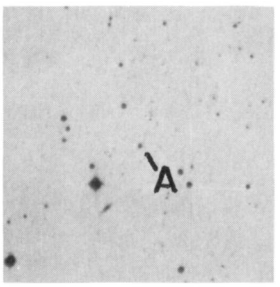

0450.3 - 1817

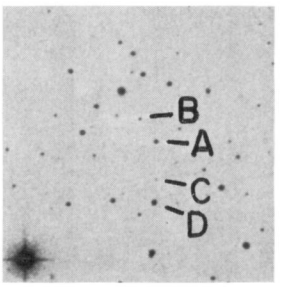

0536.3 - 2848

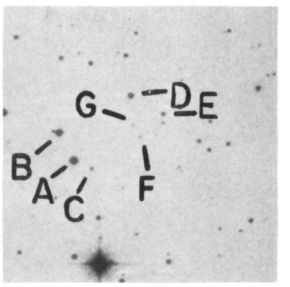

0537.1 - 2834

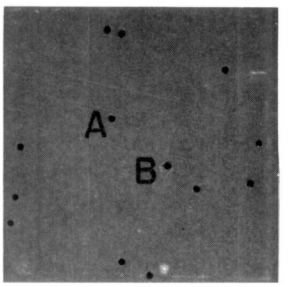

0622.5 - 5255
ESO BLUE

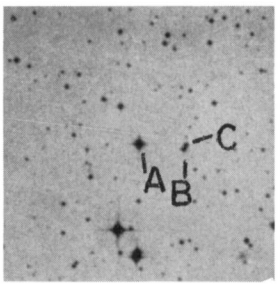

0648.1 - 5042
SRC J PLATE

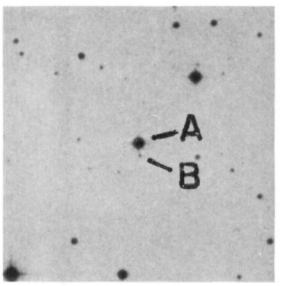

0809.8 + 4809
O PLATE

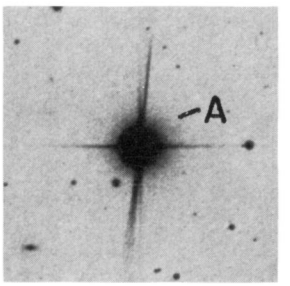

0834.7 + 6512

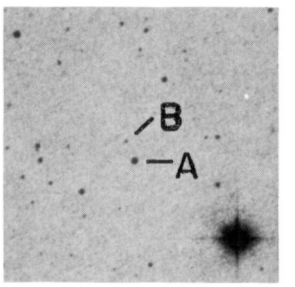

0838.6 + 1324

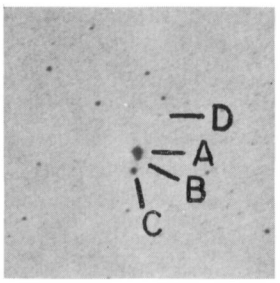

0849.0 + 2845

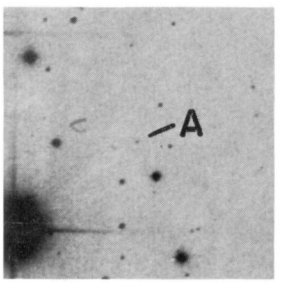

0849.2 + 2829

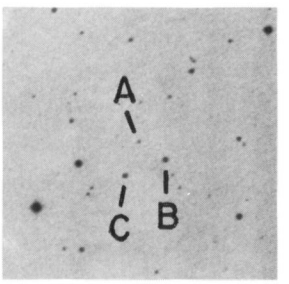

0849.8 + 2820

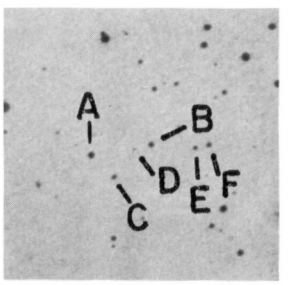

0850.0 + 2828

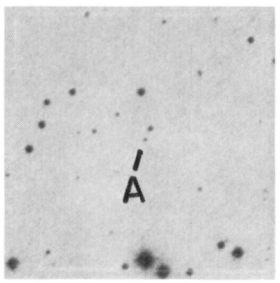

0850.2 + 2825

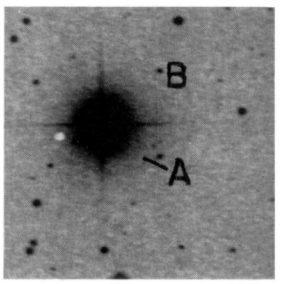

0850.9 + 1401

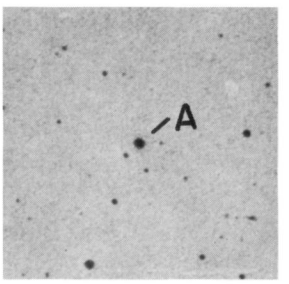

0903.5 + 1711

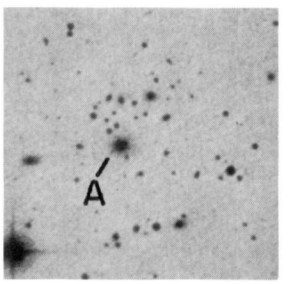

0904.5 + 1650

FIG. 1—*Continued*

STOCKE *et al.* (*see* page 459)

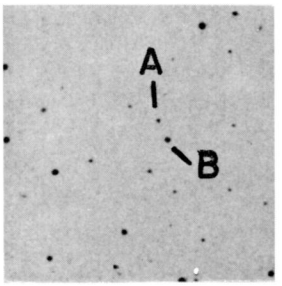

0937.8 + 1153

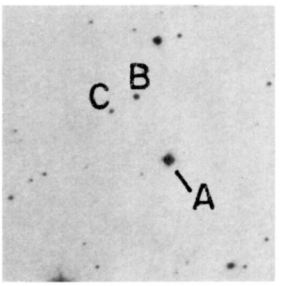

0938.3 + 1151

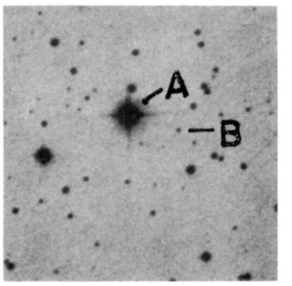

0939.8 - 2329

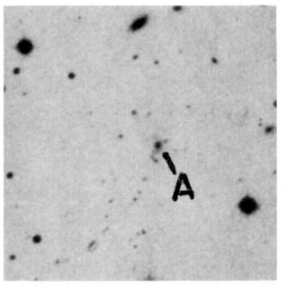

1201.5 + 2823

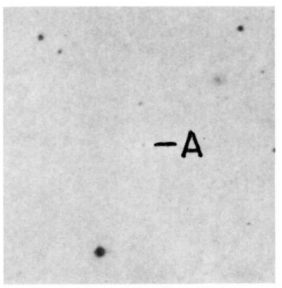

1207.9 + 3945
O PLATE

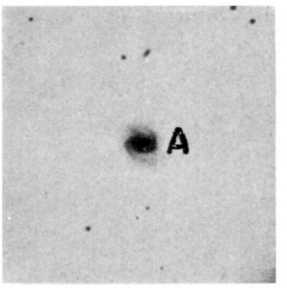

1208.3 + 3945

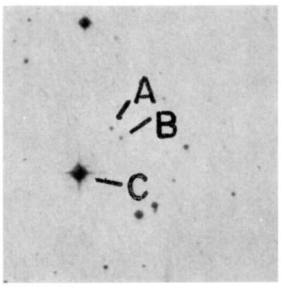

1208.7 + 3928

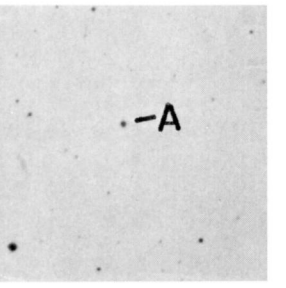

1223.5 + 2522

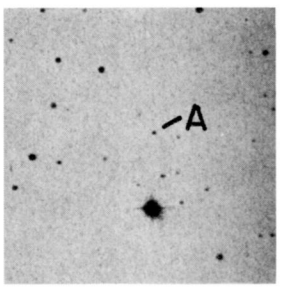

1240.8 + 0312

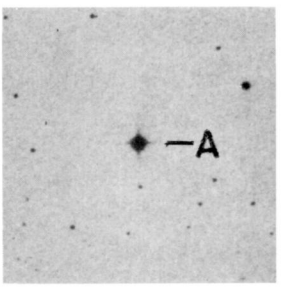

1247.0 - 0548

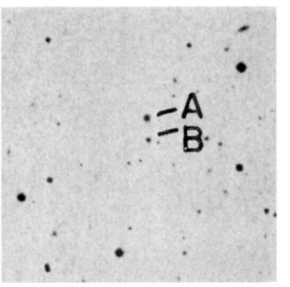

1327.4 + 3208

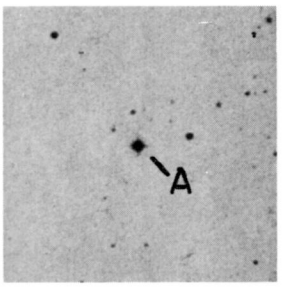

1339.9 + 6030
O PLATE

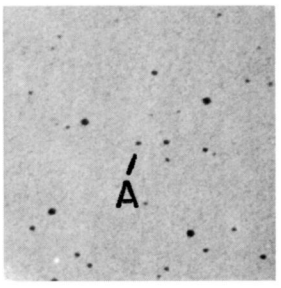

1402.3 + 0416

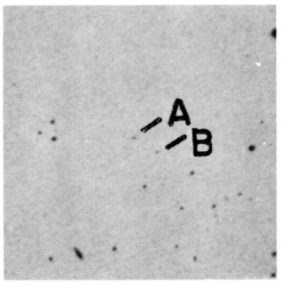

1415.0 + 2513
O PLATE

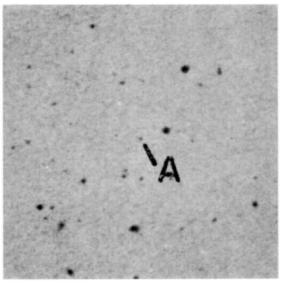

1415.1 + 2527
O PLATE

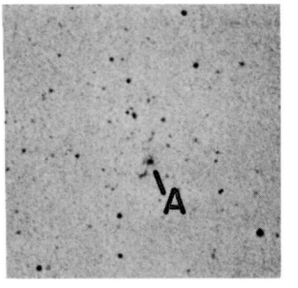

1416.2 + 2525

FIG. 1—*Continued*

STOCKE *et al.* (*see* page 459)

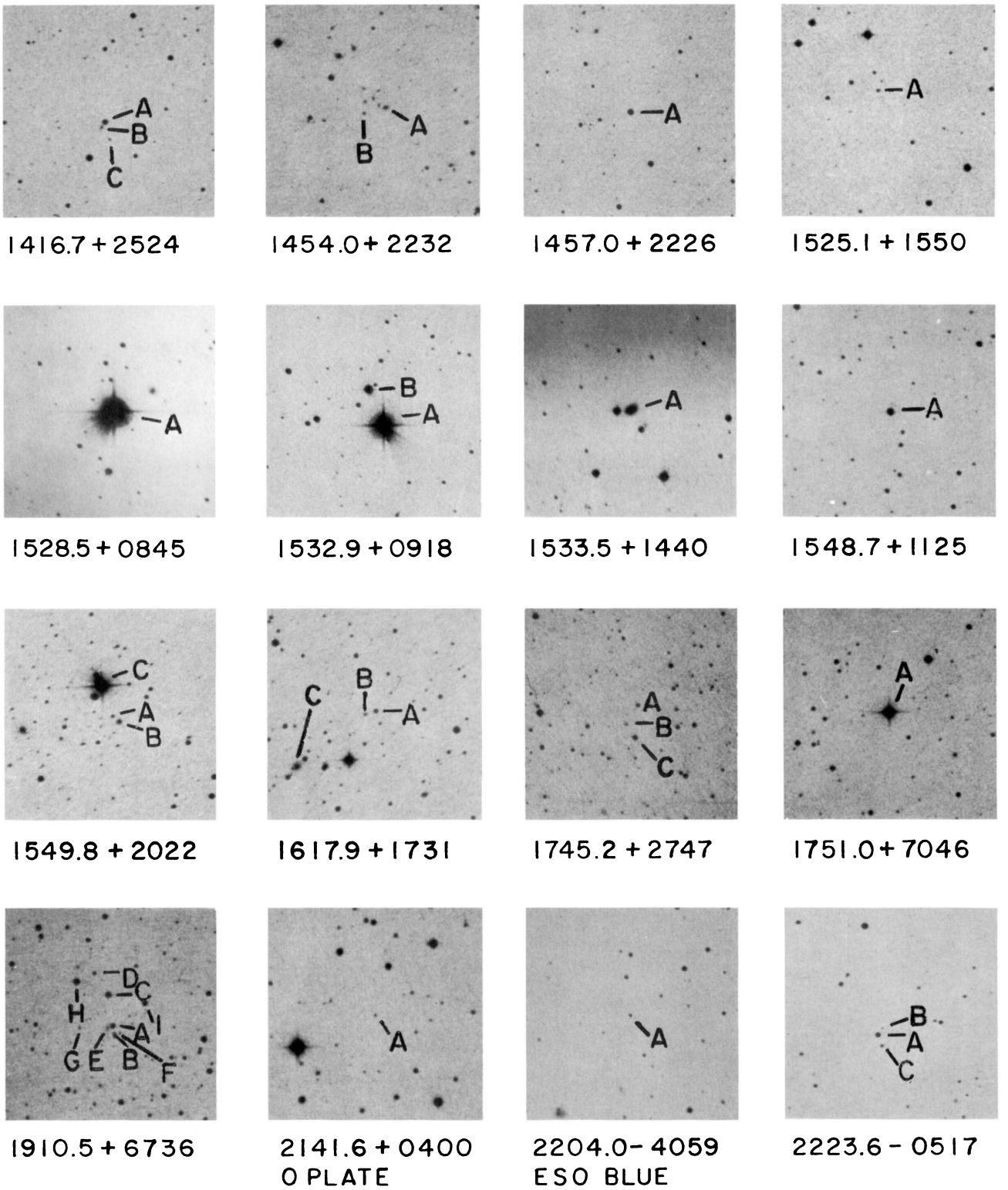

FIG. 1—*Continued*

STOCKE *et al.* (*see* page 459)